Physics Issues of Compact Drift-Optimized Stellarators

D. A. Spong, S. P. Hirshman, A. S. Ware, R. Sanchez, J. F. Lyon, L. A. Berry,
D. B. Batchelor, R. H. Fowler, W. A. Houlberg, P. Strand, D. J. Strickler, J. C. Whitson,
G. Y. Fu, D. A. Monticello, W. H. Miner, JR., P. M. Valanju, J. A. Carlsson

- Introduction/Motivation
- Optimization Method and Physics Analysis Tools
- Physics evaluations for recent configurations
  - Electron and ion neoclassical losses
  - Energetic orbit losses
  - Ballooning/kink/vertical stability
  - Bootstrap current
- Conclusions

Introduction

Compact stellarators (low A = R/<a>) offer:

- Combination of the desireable features of TOKAMAKS (low A, high β, good confinement)
- with those of the STELLARATOR

  (low recirculating power, disruption avoidance)
- Focus is on COMPACTNESS

  (while preserving confinement/stability)

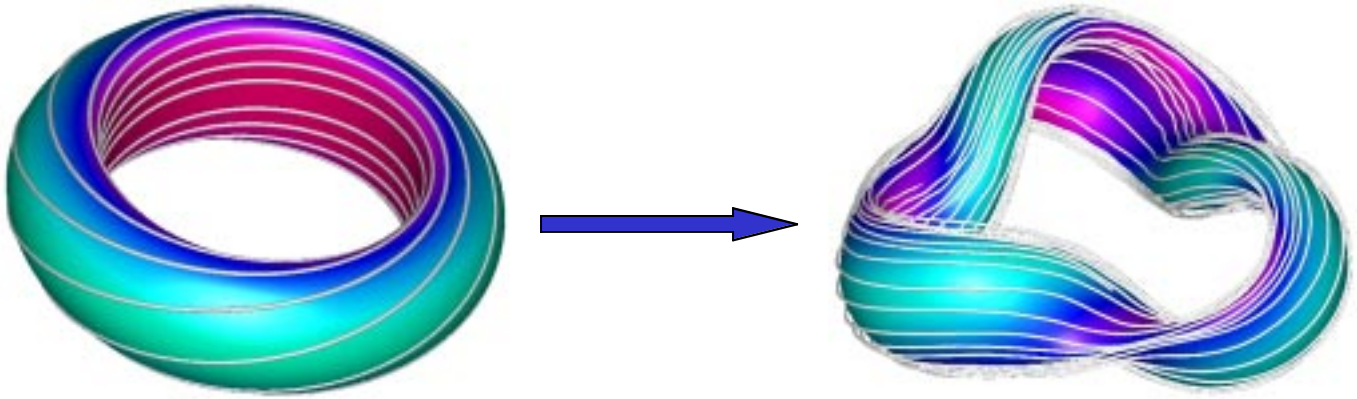

Features of low A = R/<a> stellarators

- Lower cost near-term experiments while maintaining a similar plasma radius as large aspect ratio devices
- Longer term potential of a more economically-sized, higher-power-density reactor
- Opens up a new regime of stellarator parameter space with new physics expected in:
  - transport
  - equilibrium fragility
  - plasma flow dynamics
  - enhanced confinement regimes
  - RF heating strategies
  - microturbulence

Strategies for QOS Optimization

- Optimize an ultra low aspect ratio (A = 2.5 - 3), low β configuration for a Concept Exploration experiment
  - most of the rotational transform supplied externally
- Optimize compact (A = 3 - 3.5) , high β configurations as part of the longer-term QOS program
  - a larger fraction of the transform provided by plasma currents

Methods

- Stellarator optimization
- Transport evaluation
- Ballooning
- Bootstrap Currents

Stellarator optimization loop determines outer flux surface shape. Coils to produce this shape are then "reverse-engineered":

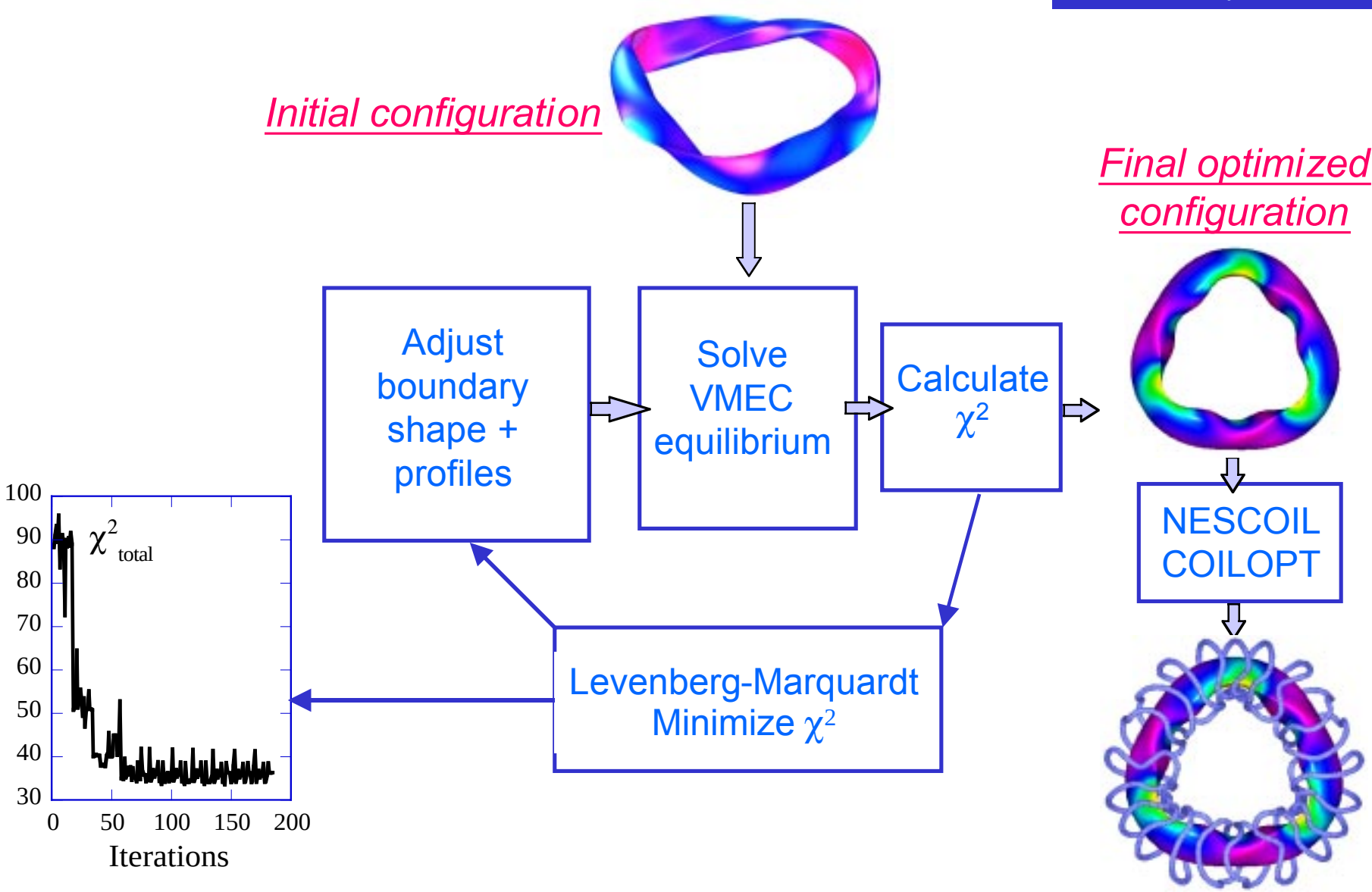

Optimization Process Successfully Integrates a complex, interacting set of Physics Criteria:

Targets (Physics/Engineering)	**Example**
Bounce-average omnigeneity (drift surfaces and flux surfaces aligned)	$B_{min} = B_{min}(\psi)$ $B_{max} = B_{max}(\psi)$ $J = J(\psi)$
Target nearby quasi-symmetries	Minimize B_{mn} if $m \neq 0$ (QP), or if $m/n \neq 1$ (QH)
Local diffusive transport	D, χ from DKES
Current profile	self-consistent I_{BS}, $I(\psi)$ goes to 0 at edge
Limit maximum plasma current	e.g., $I_{max} < 40$ kAmps
Iota profile	$i(\psi) = 0.5$ $(\rho = 0)$ to 0.8 $(\rho = a)$
Magnetic Well, Mercier	**$V'' < 0$, $D_M > 0$ over cross section**
Ballooning stability	$<\beta> \sim$ 2-4%
Aspect ratio	$R_0/a \approx$ 2.5 to 3.5
Limit outer surface curvature	avoid strong elongation/cusps

Control variables:

shape (30-40 Fourier harmonics R_{mn}, Z_{mn}) for LCFS + profile parameters

Transport optimizations using the DKES transport target have resulted in confinement improvement.

Stellarator optimization

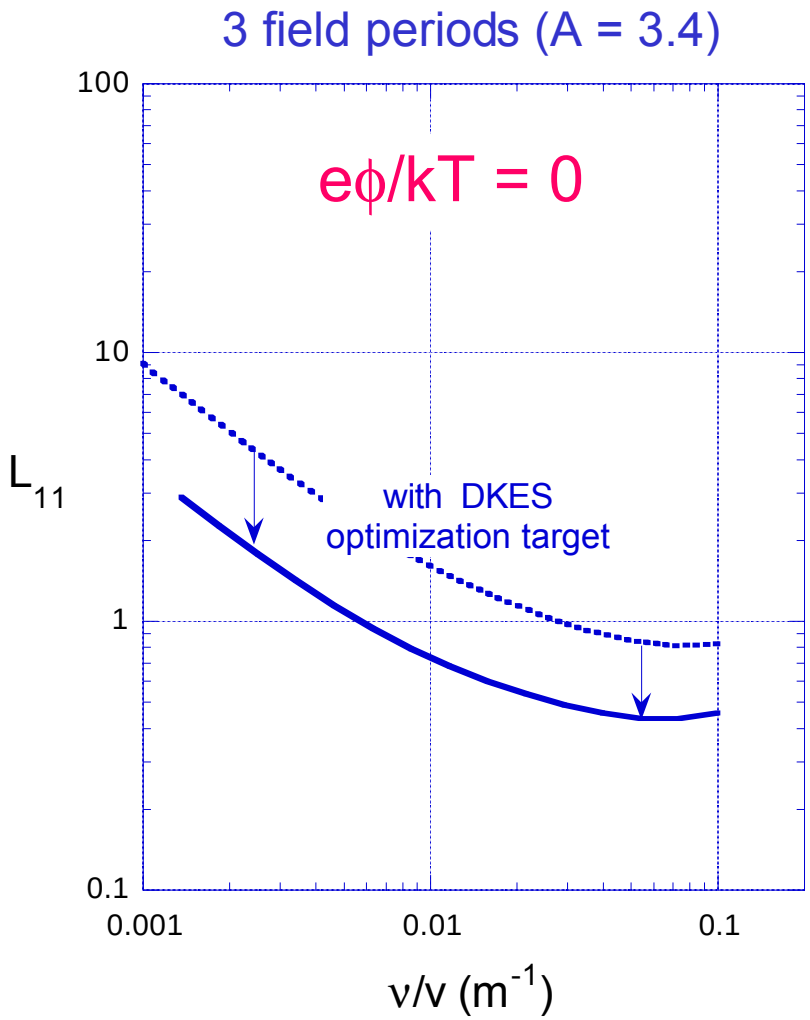

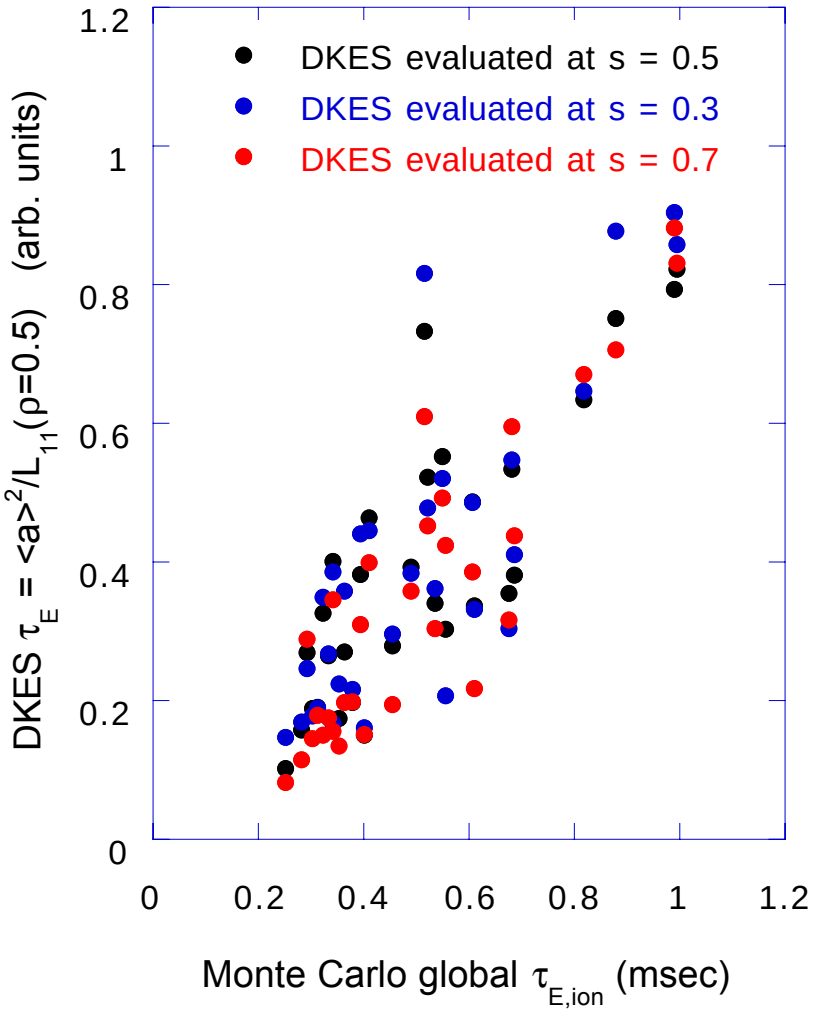

Bootstrap and Ballooning Analysis

- The COBRA code used for rapid ballooning optimization and configuration evaluation
  - Initially estimates growth rate with finite difference solution, then refines with variational principle and Richardson extrapolation
  - R. Sanchez, S.P. Hirshman, et al., Journal of Computational Physics **161**(2000) 576.
- Optimization targets collisionless bootstrap current for bootstrap consistency
  - K.C. Shaing, E.C. Crume, Jr., J.S. Tolliver, S.P. Hirshman, W.I. van Rij "Bootstrap current and parallel viscosity in the low collisionality regime in toroidal plasmas", Phys. Fluids B1, 148 (1989).
  - K.C. Shaing, S.P. Hirshman, J.S. Tolliver "Parallel viscosity-driven neoclassical fluxes in the banana regime in nonsymmetric toroidal plasmas", Phys. Fluids 29, 2548 (1986)

Transport tools

- General purpose stellarator particle simulation code (DELTA5D)
  - thermal electron/ion transport, bootstrap current
  - alpha particles
  - neutral beams, ICRH tails
  - uses MPI to achieve near linear speedup with number of processors
- Drift Kinetic Equation Solver (DKES)
  - variation of bootstrap current with collisionality and electric field
  - local diffusion coefficients → ambipolarity condition
  - integrate over profiles to obtain global lifetimes
  - uses shared memory OpenMP parallelism to achieve ~ x 3 speedup (with Ed D'Azevedo, ORNL CCS Division)
- Other qualitative measures: J, B_{min}, B_{max}, |B| contours

Applications of DKES to QO transport:

- Used in the optimizer
- Collisional bootstrap current
- Ambipolarity studies
  - Initially, use DKES for both electron and ion fluxes
  - Then hybrid model: DKES electron flux with ion particle flux from particle-based calculation

The DKES (Drift Kinetic Equation Solver) provides the full neoclassical transport coefficient matrix (multi-helicity)

$$I_i = \begin{bmatrix} \vec{\Gamma} \bullet \vec{\nabla} s \\ \frac{1}{T} \vec{Q} \bullet \vec{\nabla} s \\ n \left\langle (\vec{u} - \vec{u}_s) \bullet \vec{B} \right\rangle \end{bmatrix} = -\sum_{j=1}^{3} L_{ij} A_j \qquad A_j = \begin{bmatrix} \frac{n'}{n} - \frac{3}{2}\frac{T'}{T} - \frac{eE_r}{T} \\ \frac{T'}{T} \\ -\left(\frac{e}{T}\right)\left(\frac{\left\langle \vec{E} \bullet \vec{B} \right\rangle}{\left\langle B^2 \right\rangle}\right) \end{bmatrix}$$

$$L_{ij} = n \frac{2}{\sqrt{\pi}} \int_0^\infty dK \sqrt{K}\, e^{-K} g_i g_j D_{ij}$$

where $g_1 = g_3 = 1,\ g_2 = K, \quad K = \left(\frac{v}{v_{th}}\right)^2$

$$D_{11} = D_{12} = D_{21} = D_{22} = -\frac{v_{th}}{2}\left[\frac{B v_{th}}{\Omega}\left(\frac{d\rho}{dr}\right)^{-1}\right]^2 K\sqrt{K}\ \Gamma_{11}$$

$$D_{31} = D_{32} = -D_{13} = -D_{23} = -\frac{v_{th}}{2}\left[\frac{B v_{th}}{\Omega}\left(\frac{d\rho}{dr}\right)^{-1}\right] K\ \Gamma_{31}$$

$$D_{33} = -\frac{v_{th}}{2}\sqrt{K}\ \Gamma_{33}$$

$$\Gamma_{ij} = \Gamma_{ij}\left(\frac{\nu}{v}, \frac{E_r}{v}\right)$$

- W. I. Van Rij, S. P. Hirshman, Phys. Fluids **B 1**, 563 (1989)
- Variational: provides upper and lower bounds on dS/dt
- Expands f in Fourier-Legendre series

(i.e., to carry out the above integrals, one will need to generate a 2-D matrix of Γ's vs. these parameters for each flux surface)

DELTA5D Monte Carlo code is used for both thermal plasma and fast ion confinement studies

Transport analysis

- Thermal plasma
  - Global and local diffusive limits
- Various fast ion populations
  - ICRF tails (quasilinear diffusion operator)
  - Neutral beam ions (pencil beam approximation)
  - Alphas
  - Alfvén turbulence (to be added)
- Options for f and δf particle weightings
- Diagnostics: particle and energy losses, loss patterns, energy slowing down, escaping pitch angle/energy/lifetime distributions
- Longer term goal: Multi-species (thermal, fast ion, impurity), coupled transport and electric field evolution model
- Computational characteristics
  - parallelization over particles rather than domains
  - uses collective MPI communications, runs on T3E and IBM-SP

Hamiltonian Guiding Center Orbit Equations:

Transport analysis

$$\dot{\psi} = \left(g\dot{P}_\theta - I\dot{P}_\phi\right)/D, \qquad \dot{\rho}_\| = \frac{1}{D}\left[-(\rho_\| g' - \iota)\dot{P}_\theta + (1+\rho_\| I')\dot{P}_\phi\right]$$

$$\dot{\theta} = \left\{\left[\frac{e^2\rho_\|^2 B}{m} + \mu\right]\frac{\partial B}{\partial \psi} + e\frac{\partial \Phi}{\partial \psi}\right\}\frac{\partial \psi}{\partial P_\theta} + \frac{e^2B^2}{m}\rho_\|\frac{\partial \rho_\|}{\partial P_\theta}$$

$$\dot{\phi} = \left\{\left[\frac{e^2\rho_\|^2 B}{m} + \mu\right]\frac{\partial B}{\partial \psi} + e\frac{\partial \Phi}{\partial \psi}\right\}\frac{\partial \psi}{\partial P_\phi} + \frac{e^2B^2}{m}\rho_\|\frac{\partial \rho_\|}{\partial P_\phi}$$

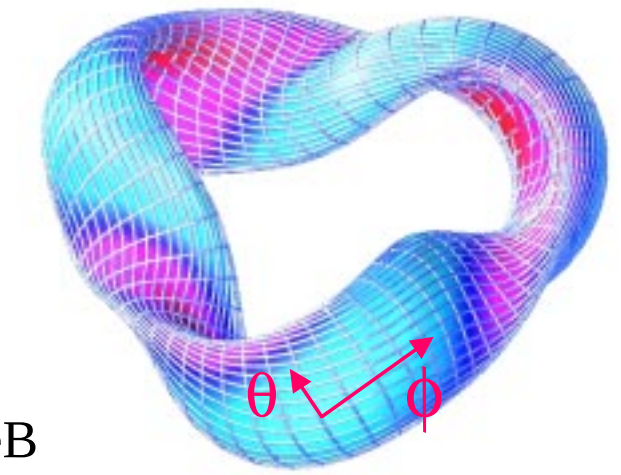

where $D = e\left[g + \iota I + \rho_\|(gI' - Ig')\right], \qquad \rho_\| = mv_\| / eB$

$$\dot{P}_\theta = -\frac{\partial B}{\partial \theta}\left[\frac{e^2\rho_\|^2 B}{m} + \mu\right], \qquad \frac{\partial \rho_\|}{\partial P_\theta} = -(\rho_\| g' - \iota)/D$$

$$\dot{P}_\phi = -\frac{\partial B}{\partial \phi}\left[\frac{e^2\rho_\|^2 B}{m} + \mu\right], \qquad \frac{\partial \rho_\|}{\partial P_\phi} = (I'\rho_\| + 1)/D$$

Φ = electrostatic potential
g = net poloidal current outside a flux surface
I = net toroidal current inside a flux surface
ι = rotational transform

Coulomb collision operator for collisions of test particles (a) with a background plasma (b):

$$C_{ab} f_a = \frac{\nu_D^{ab}}{2} \frac{\partial}{\partial \lambda} (1-\lambda^2) \frac{\partial f_a}{\partial \lambda} + \frac{1}{v^2} \frac{\partial}{\partial v} \left\{ v^2 \left[2\nu_\varepsilon \alpha_{ab} f_a + \frac{\nu_\varepsilon}{v} \alpha_{ab}^3 \frac{\partial f_a}{\partial v} \right] \right\}$$

where

$$\nu_D^{ab} = \frac{\nu_0^{ab}}{(v/\alpha_{ab})^3} \left[\phi\left(\frac{v}{\alpha_b}\right) - G\left(\frac{v}{\alpha_b}\right) \right] \qquad \nu_\varepsilon = \nu_0^{ab} G\left(\frac{v}{\alpha_b}\right)$$

$$\phi(x) = \frac{2}{\sqrt{\pi}} \int_0^x dt\ t^{1/2}\ e^{-t} \qquad G(x) = \frac{1}{2x^2} [\phi(x) - x\phi'(x)]$$

$$\alpha_{ab} = \sqrt{\frac{2T_{b0}}{m_a}} \qquad \alpha_b = \sqrt{\frac{2T_{b0}}{m_b}} \qquad \nu_0^{ab} = \frac{4\pi m_b \ln \Lambda_{ab} (e_a e_b)^2}{(2T_b)^{3/2} m_a^{1/2}}$$

Monte Carlo Equivalent of the Fokker-Planck Operator

[A. Boozer, G. Kuo-Petravic, Phys. Fl. **24** (1981)]

Transport analysis

$$\lambda_n = \lambda_{n-1}(1-\nu_d \Delta t) \pm \left[\left(1-\lambda_{n-1}^2\right)\nu_d \Delta t\right]^{1/2}$$

$$E_n = E_{n-1} - (2\nu_\varepsilon \Delta t)\left[E_{n-1} - \left(\frac{3}{2} + \frac{E_{n-1}}{\nu_\varepsilon}\frac{d\nu_\varepsilon}{dE}\right)T_b\right] \pm 2\left[T_b E_{n-1}\nu_\varepsilon \Delta t\right]^{1/2}$$

Local Monte-Carlo equivalent quasilinear ICRF operator (developed by J. Carlsson)

$$E^{+} = E^{-} + \mu^{E} + \zeta\sqrt{\sigma^{EE}} \qquad \lambda^{+} = \lambda^{-} + \mu^{\lambda} + \zeta\sqrt{\sigma^{\lambda\lambda}}$$

Transport analysis

$\zeta = \text{a zero-mean, unit-variance random number (i.e., } \mu^{\zeta} = 0 \text{ and } \sigma^{\zeta} = 1)$

$$\sigma^{EE} = 2\,m^2 v_\perp^2 \Delta v_0 \qquad \sigma^{\lambda\lambda} = 2\left(\frac{k_\parallel}{\omega} - \frac{v_\parallel}{v^2}\right)^2 \frac{v_\perp^3 \Delta v_0}{v^2}$$

$$\mu^{E} = 2\left(1 - \frac{k_\parallel v_\parallel}{\omega}\right) m v_\perp \Delta v_0 \qquad \mu^{\lambda} = \left\{2\left[\left(1 - \frac{k_\parallel v_\parallel}{\omega}\right) - \frac{v_\perp^2}{v^2}\right]\left(\frac{k_\parallel}{\omega} - \frac{v_\parallel}{v^2}\right) + \frac{v_\parallel}{v^2}\frac{v_\perp^2}{v^2}\right\}\frac{v_\perp \Delta v_0}{v}$$

where

$$\Delta v_0 = \frac{1}{v_\perp}\left(\frac{eZ}{2m}\left|E_{+}J_{n-1}(k_\perp\rho) + E_{-}J_{n+1}(k_\perp\rho)\right|\right)^2 \frac{2\pi}{n|\dot{\Omega}|}$$

as $\dot{\Omega} \to 0$

$$\frac{2\pi}{n|\dot{\Omega}|} \to 2\pi^2\left|\frac{2}{n\ddot{\Omega}}\right|^{2/3} \times \mathrm{Ai}^2\left(-\frac{n^2\dot{\Omega}^2}{4}\left|\frac{2}{n\ddot{\Omega}}\right|^{4/3}\right)$$

For the low density, higher temperature case, the ion particle density evolves to a hollow profile shape.

Transport analysis

In future work will explore dependence on:

- Particle refueling and energy input model
- Self-consistency between collision operator and particle profiles

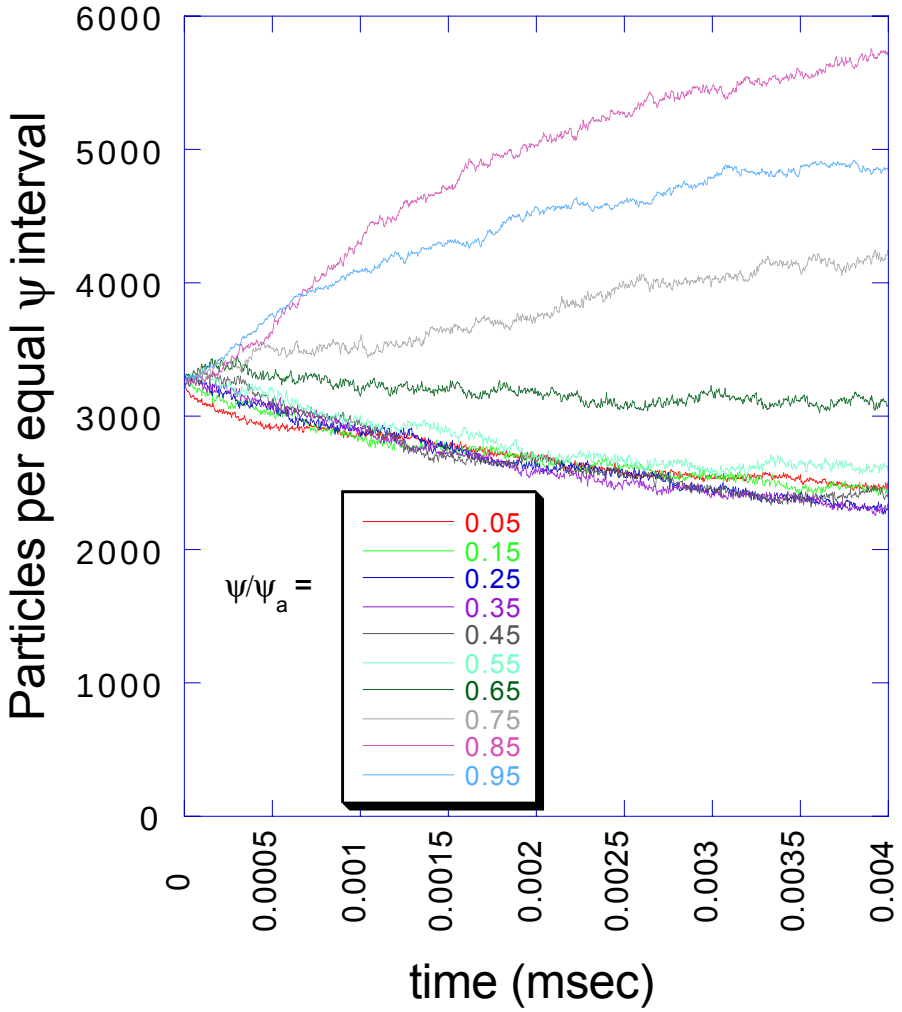

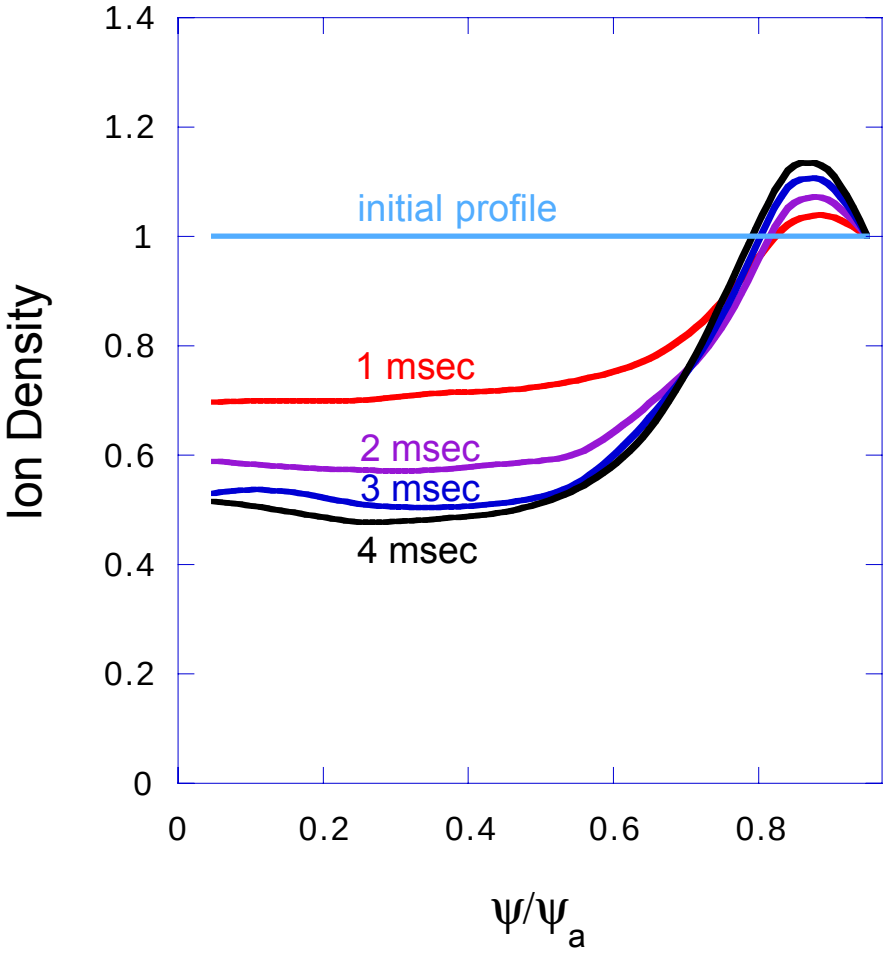

Particle fluxes are peaked near the center where the ion temperature is highest

$n(0) = 3 \times 10^{13}$ cm^{-3}, $T(0) = 1.8$ keV

time-averaged ion particle fluxes

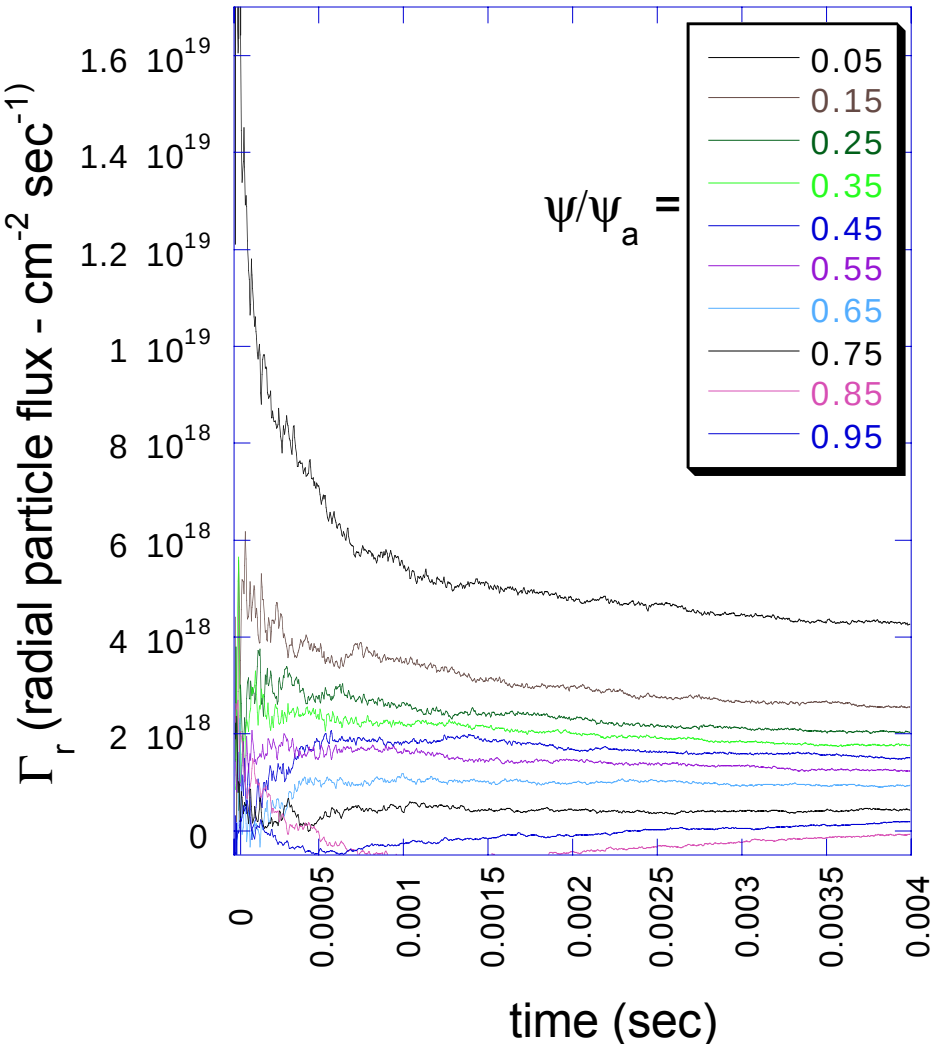

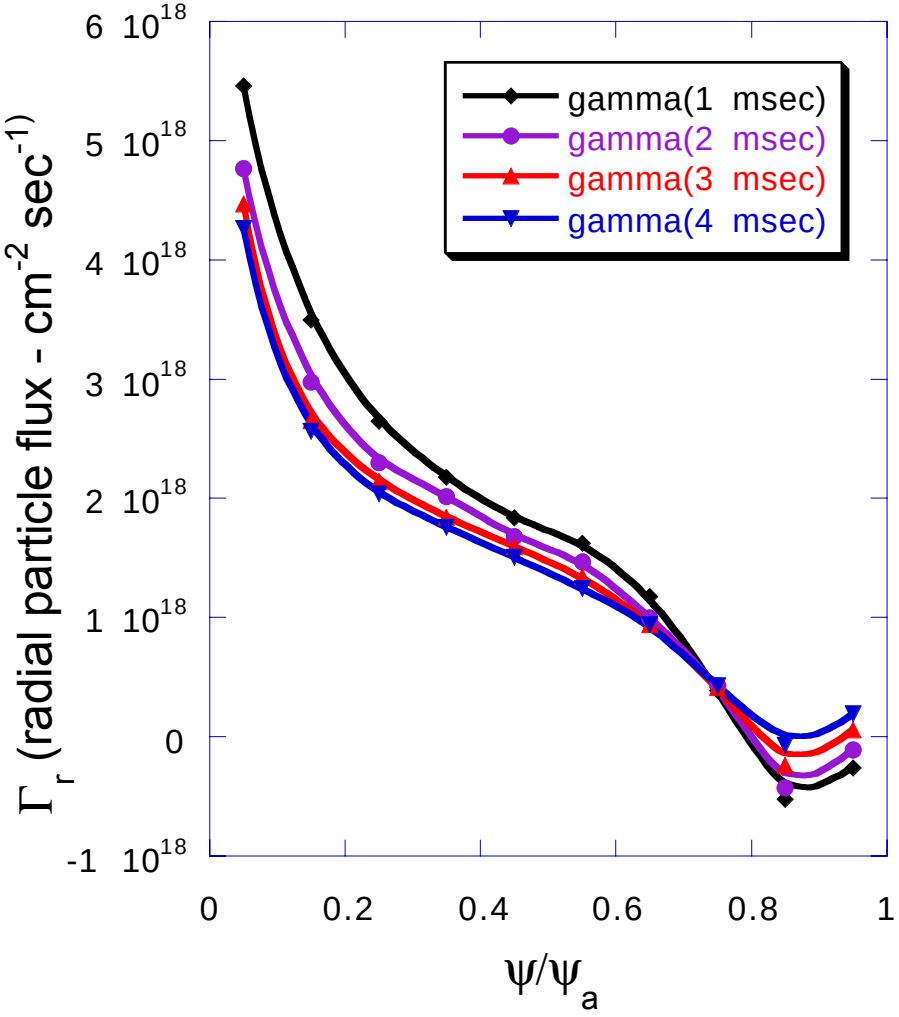

Since ICRF heating does not preserve μ or J, it can enhance radial particle fluxes. This can be an important issue and control knob for the generation of the ambipolar electric field

Transport analysis

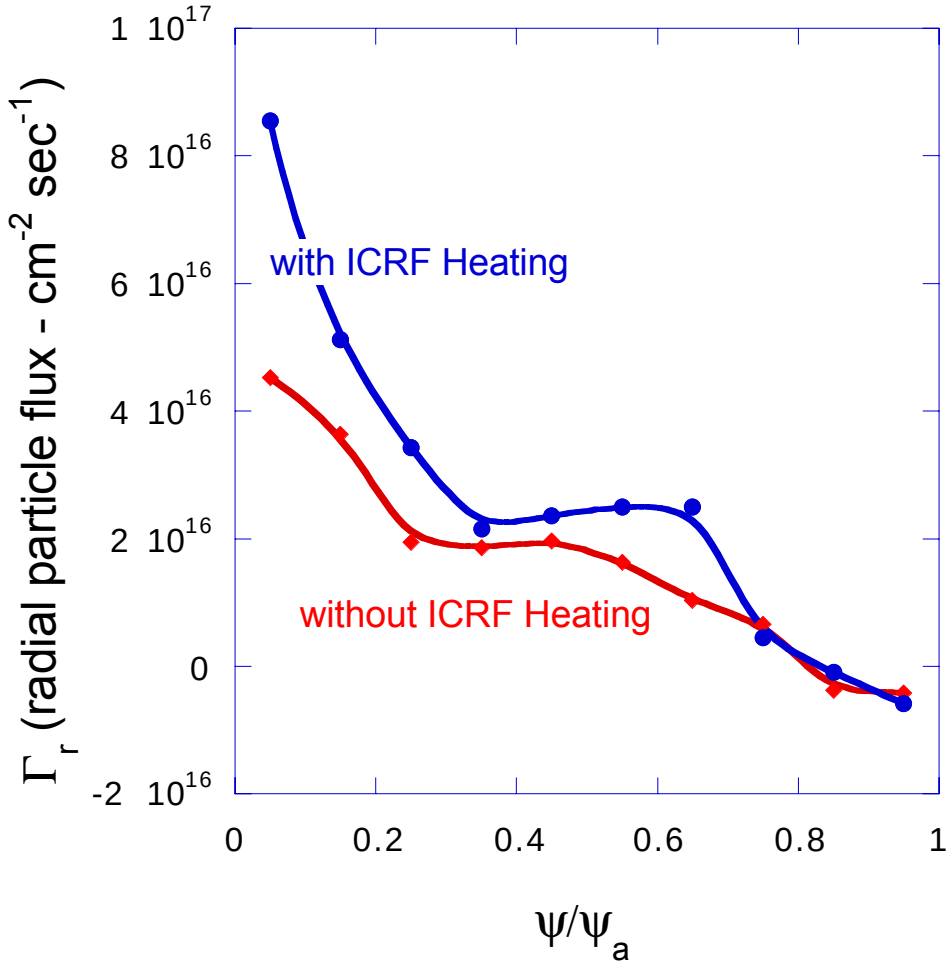

Configuration Development

- Ultra low A (2.5 - 3), near-term devices
  - most of the transform supplied externally
  - quasi-poloidal symmetry built-in
- Compact (A = 3 - 3.5) high β devices
  - large fraction of transform comes from current
  - quasi-poloidal symmetry enhanced by high β

Selection Criteria for Configurations

- Guidelines for the selection of a configuration for a CE:
  - Compact: A < 3
    - This ultra low aspect ratio range is lower than existing stellarators (1/2 to 2/3 that of NCSX)
  - Good confinement: $\tau_{neo} > 2*\tau_{ISS95}$
    - Drift-optimized so that neoclassical transport is not the dominant loss mechanism
    - Cases normalized to: $R \cdot \langle a \rangle = 0.278$ and $\langle | B | \rangle = 1.0$

Selection Criteria for Configurations (cont.)

- Stability: MHD stable at $\beta \sim 2\%$
  - Ballooning and Mercier analysis included in optimization to ensure stability at β levels relevant to a CE
- Accessibility: not an issue for low I_{BS} QOS
- Flexibility: ability to vary the bootstrap current through the |B|-spectrum

Quasi-Poloidally Symmetric Cases

Equilibrium

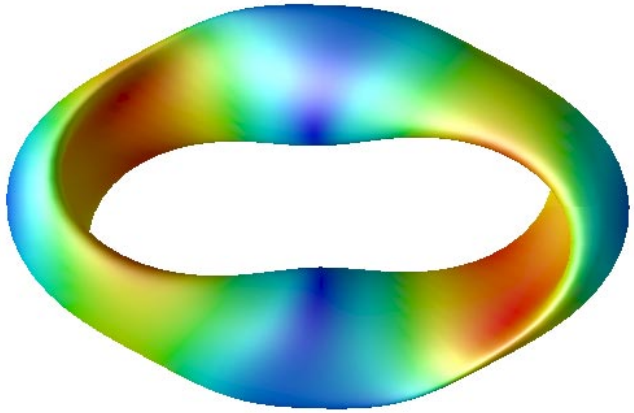

- Base case: A2.5_M2_B1.3
  - Max.Tor.Cur. = 25.7 kA
- Low aspect ratio: A < 2.5
  - Have obtained configurations with aspect ratios in the range: A=2.1 to A=3.0
- Rotational transform below 0.5: $\iota \sim 0.3 - 0.4$
  - Majority of the transform is from the coils, bootstrap current causes iota to increase
  - Stable to neoclassical tearing modes

Outer Surface Views for A2.5_M2_B1.3

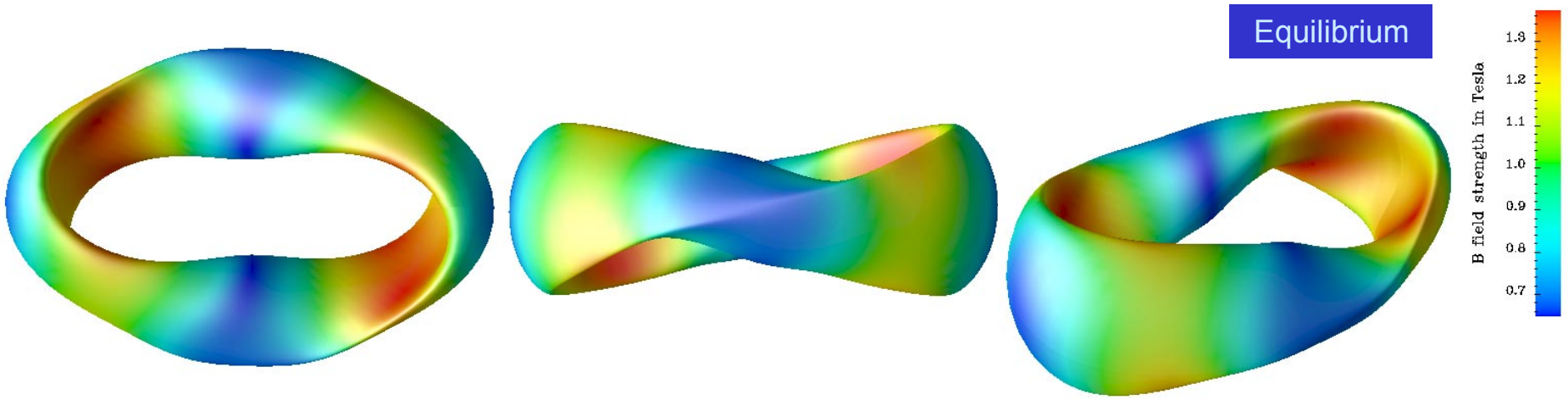

Cross Sections for A2.5_M2_B1.3

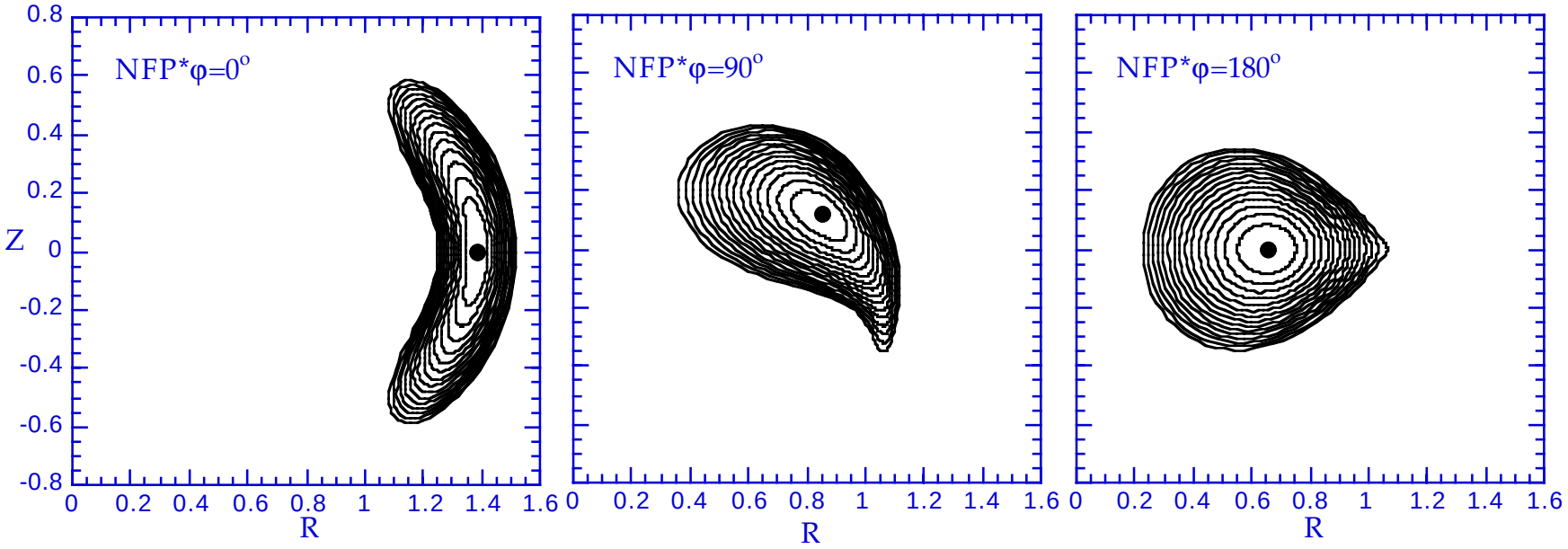

Free boundary A2.5_M2_B1.3 configuration (from coils) yields very similar transport as original fixed boundary case:

green = free boundary

blue = fixed boundary

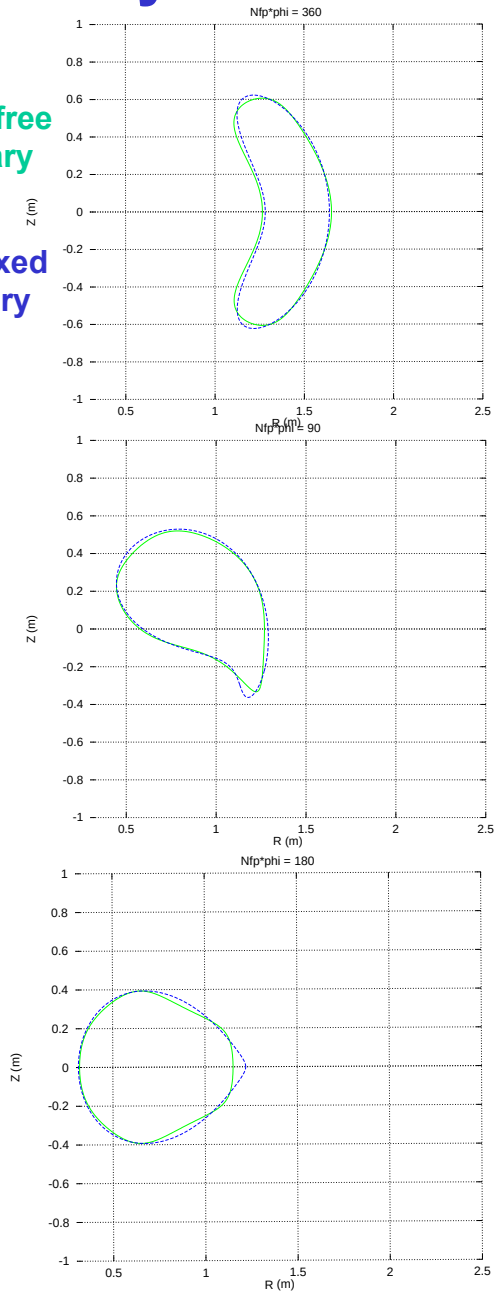

Transport analysis

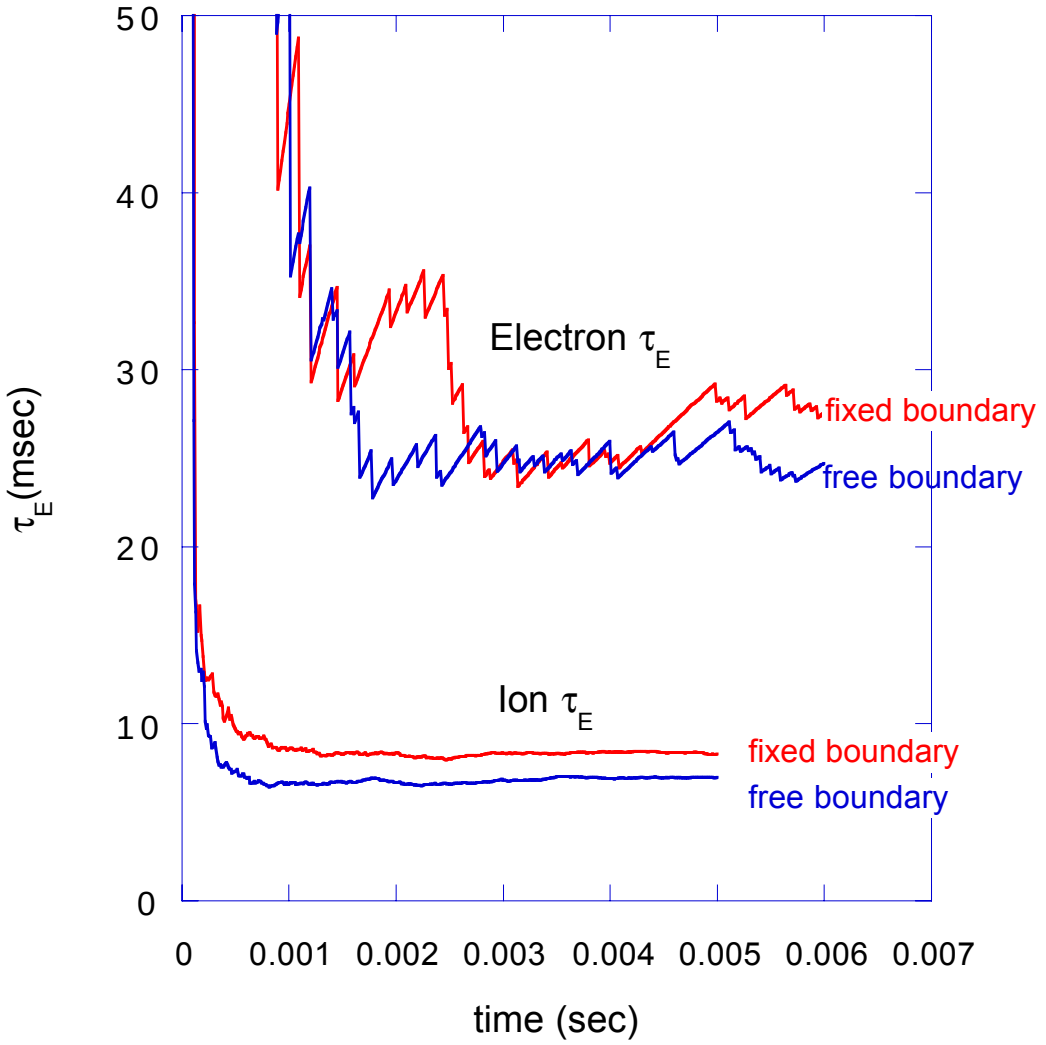

Profiles used in transport studies

- n = constant, Z_{eff} = 1
- $(1 - r^2)^2$ T_e, T_i profiles
- $e\phi(r)$ varies inversely with kT_e
- ion root
- electron root to be investigated

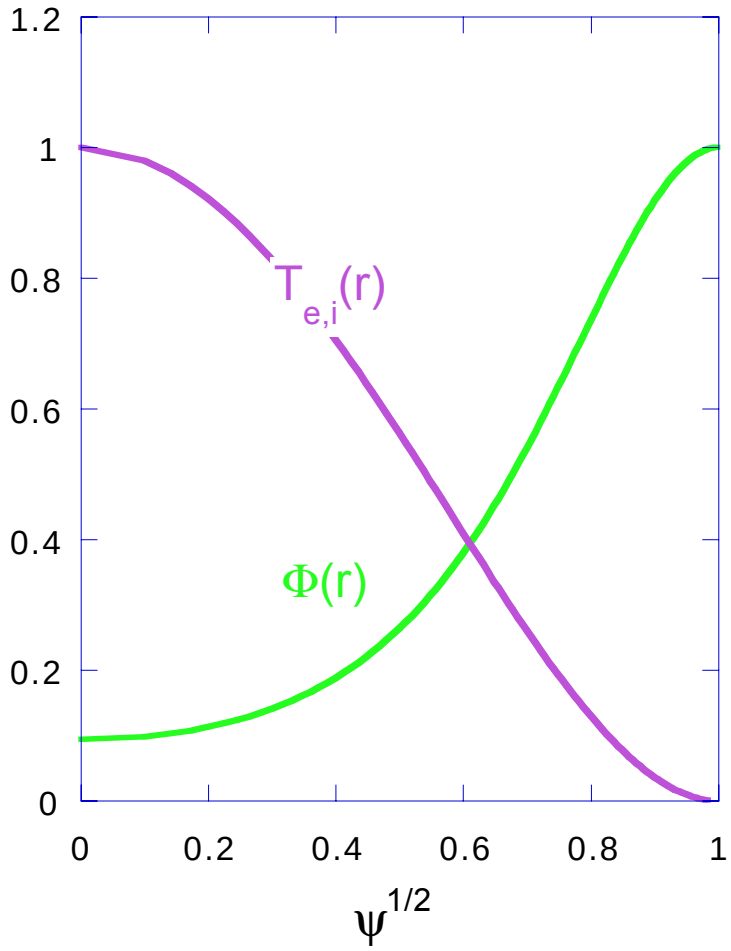

Projected QO/CE heating scenarios include both ECH and ICH regimes

Transport analysis

RF	P_{heat} (MW)	<B> (Tesla)	$n/10^{20}$ (m^{-3})	T_e (keV)	T_i (keV)	τ_{ISS95} (msec)	ν_{*elec}	ν_{*ion}	<β>
(1) ECH	**0.5**	**1**	**0.18**	**1.4**	**0.15**	**8.1**	**0.019**	**1.6**	**0.7**
(2) ECH	**1**	**0.5**	**0.045**	**2.1**	**0.2**	**1.5**	**0.0021**	**0.22**	**1**
(3) ICH	**1**	**1**	**0.83**	**0.5**	**0.5**	**11.7**	**0.68**	**0.64**	**2**
(4) ICH	**1**	**0.5**	**0.59**	**0.4**	**0.25**	**5.5**	**0.75**	**1.8**	**3.7**

Confinement in the 2 field period, A = 2.5 configuration covers a range from $\tau_{E,global}$ = (1.4 to 3.6) $\tau_{E,ISS95}$ for different ECRF and ICRF heating scenarios

Transport analysis

RF	B (Tesla)	τ_E^{ion} ($msec$)	τ_E^{elec} ($msec$)	τ_E^{global} ($msec$)	τ_E^{ISS95} ($msec$)
ECH	1	16.2	17.4	16.2	8.1
ECH	0.5	4.27	1.95	2.1	1.5
ICH	1	27	~100	41.7	11.7
ICH	0.5	7.7	~55	16.4	5.5

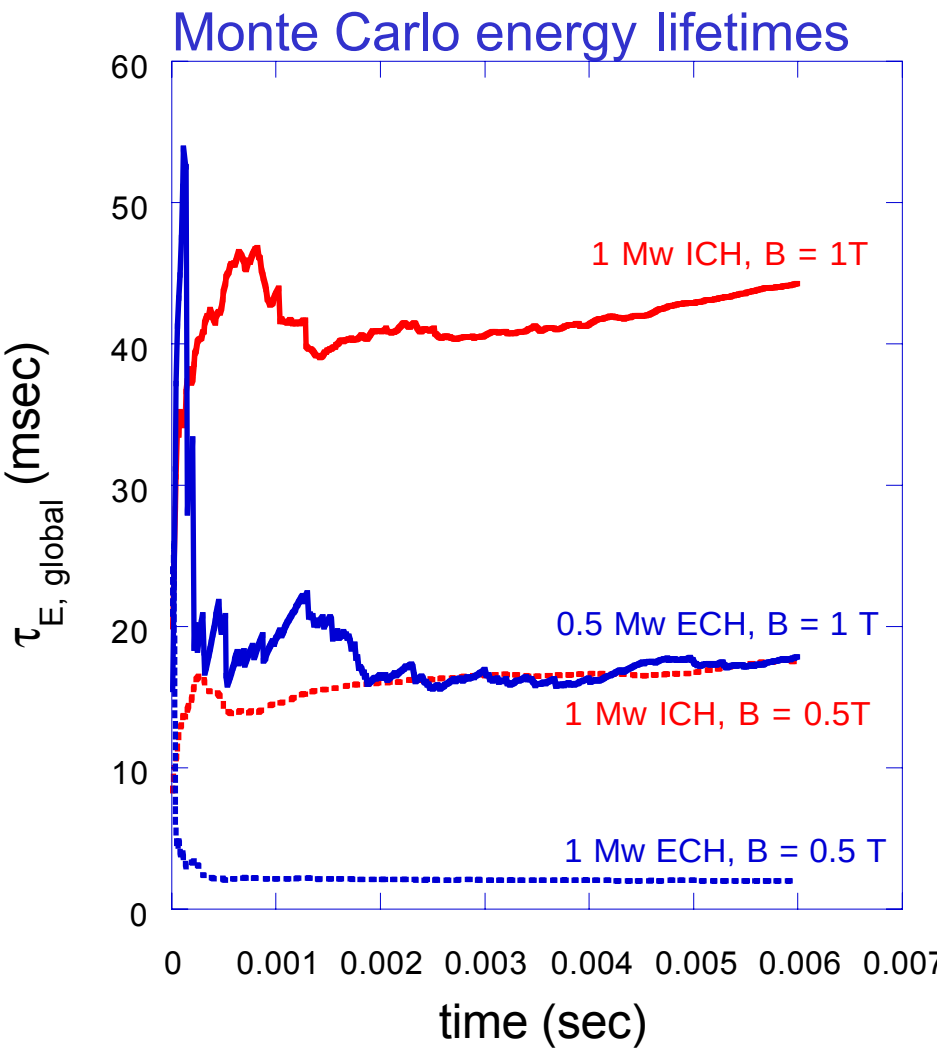

Transport analysis in regimes with ($T_e > T_i$) for the 2 field period A=2.5 device shows tendency to improve with increasing β:

T_e = 1.8 keV, T_i = 0.5 keV, n = 3 x 10^{13} cm^{-3}

ν_{*e} = 0.019, ν_{*i} = 0.233

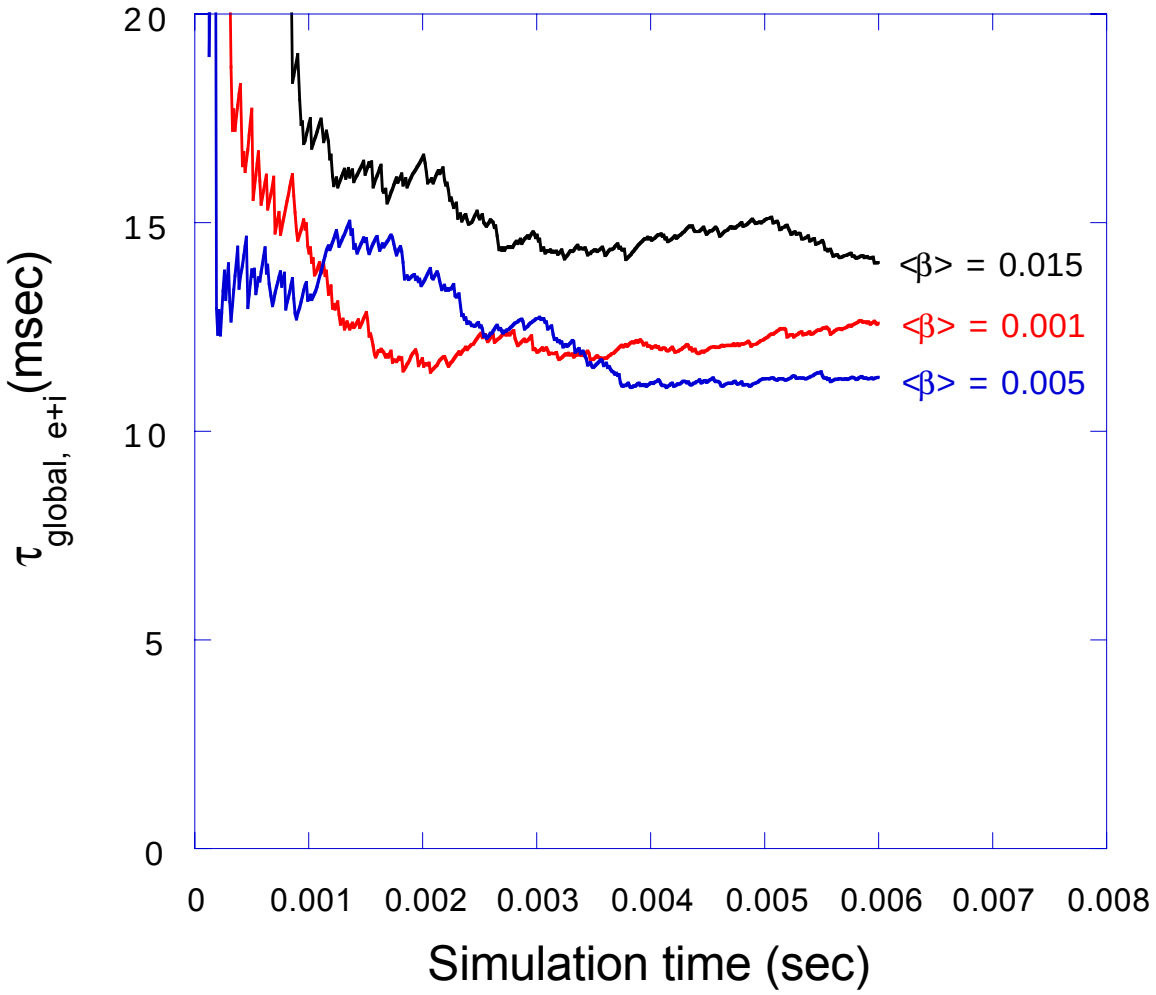

Energetic particle loss simulations show exit pitch angle, energy and exit position of ions on outer flux surface

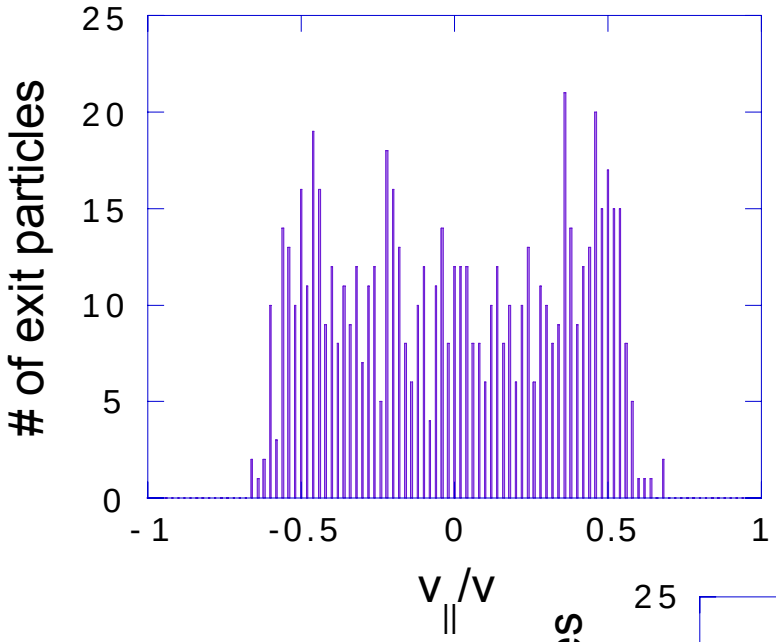

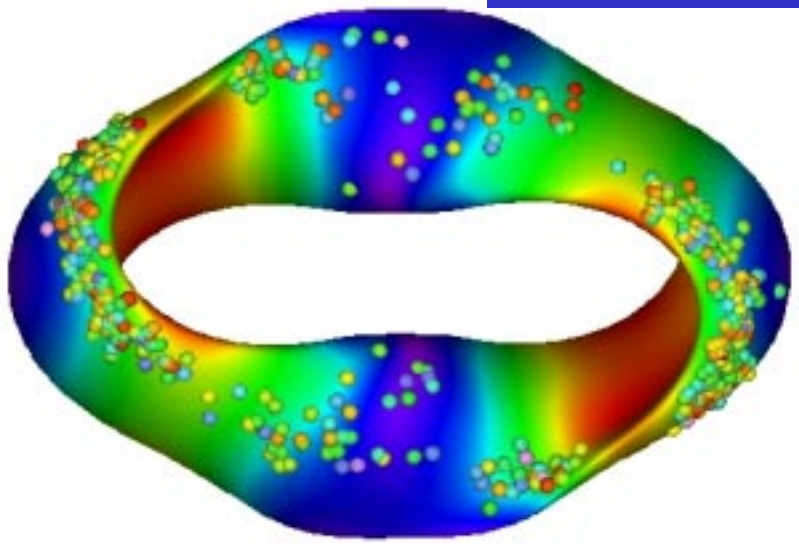

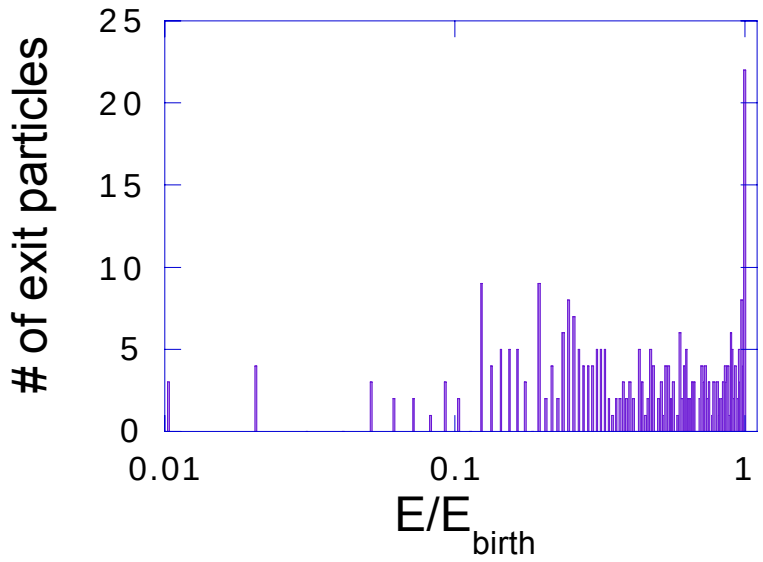

Collisionality and electric field dependence of bootstrap current coefficient (results shown are for N_{fp} = 2, A = 2.5 device)

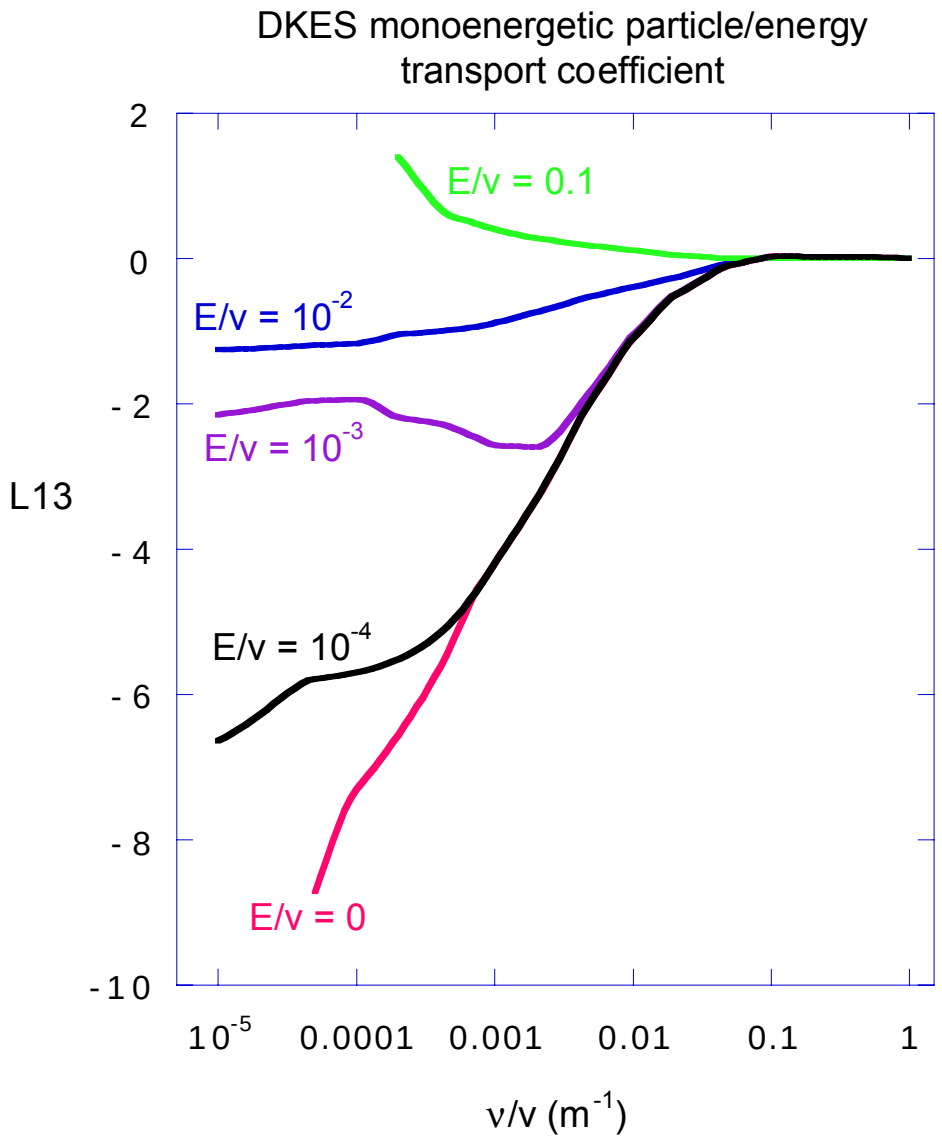

Self-Consistent ambipolar electric field calculations

- initially DKES will be used offline for electrons and ion to obtain $\phi(r)$ for DELTA5D
- next step is to use DKES for electron flux coupled with DELTA5D for ion flux

Transport analysis

Ion, electron fluxes from DKES

$$\Gamma_i = -L_{11}^i(E_r)\left[\frac{n'}{n} - \frac{3}{2}\frac{T'}{T} - \frac{ZeE_r}{T}\right] - L_{12}^i(E_r)\frac{T'}{T}$$

$$\Gamma_e = -L_{11}^e(E_r)\left[\frac{n'}{n} - \frac{3}{2}\frac{T'}{T} + \frac{eE_r}{T}\right] - L_{12}^e(E_r)\frac{T'}{T}$$

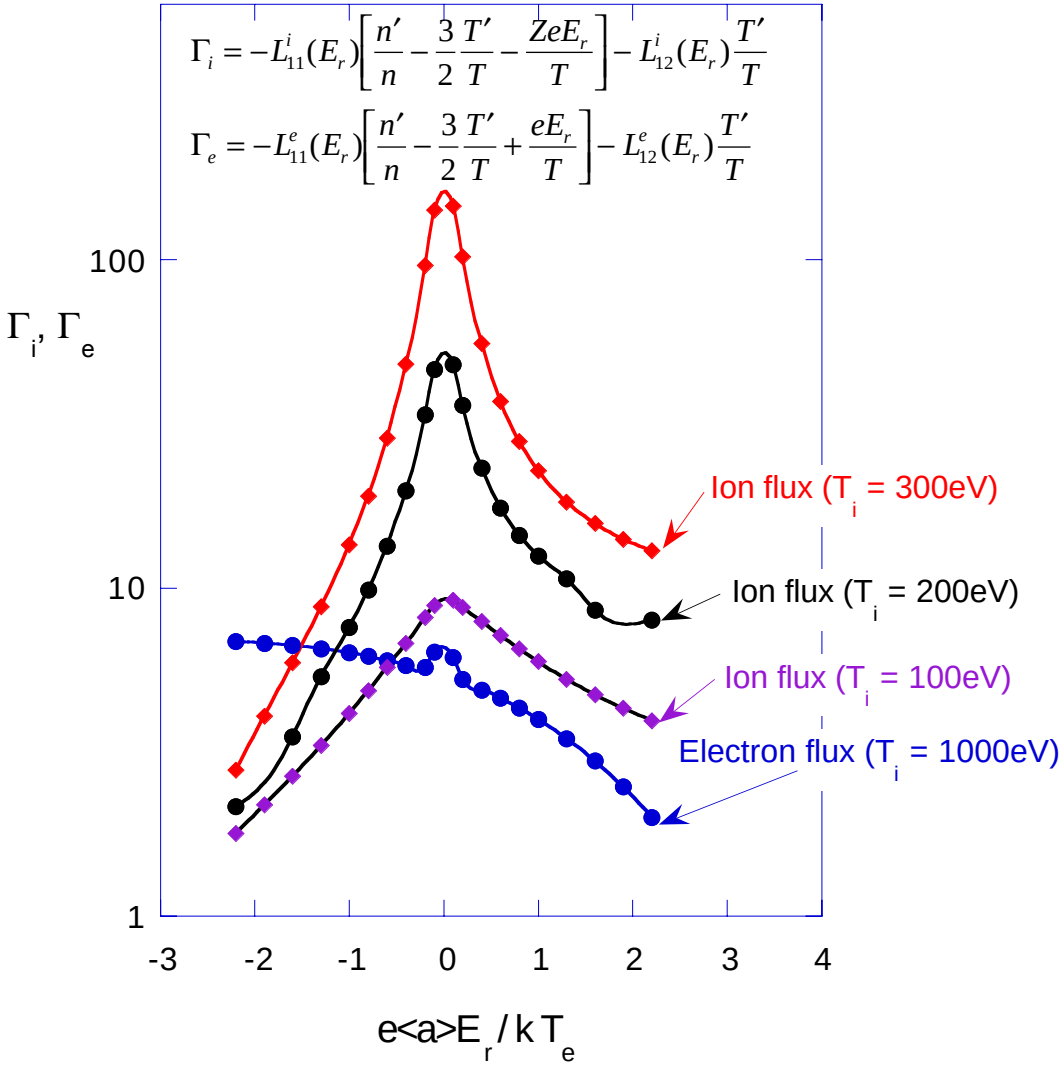

Ion flux from DELTA5D

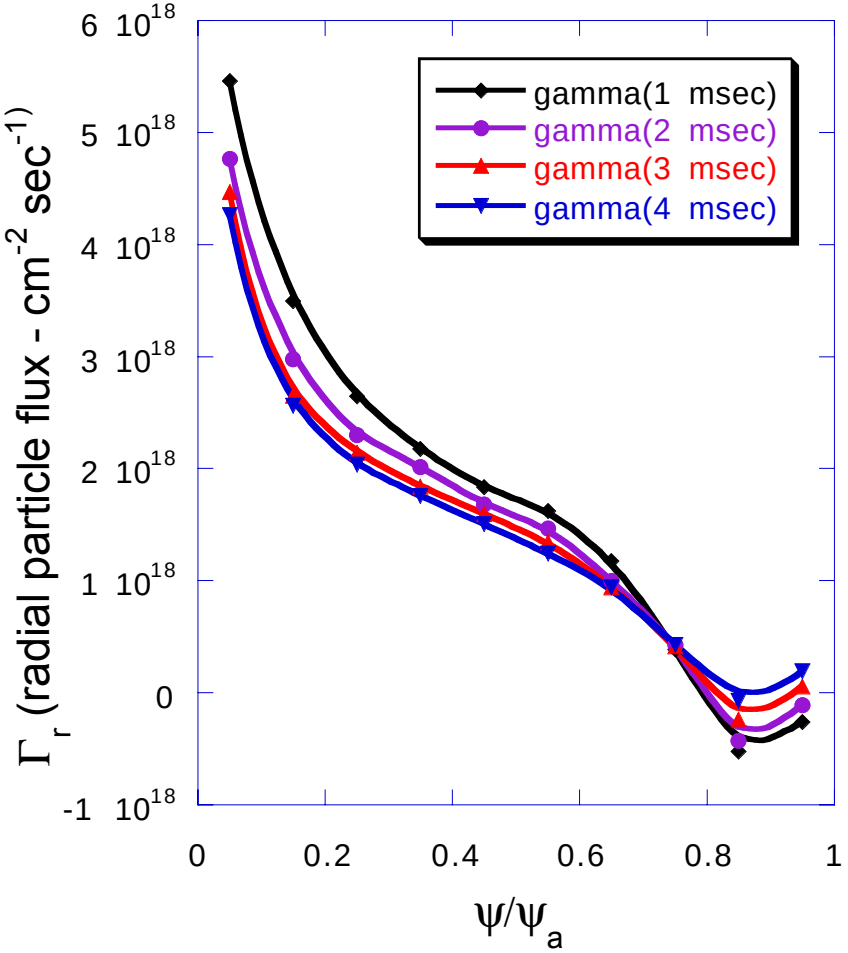

QP Symmetry Cases (cont.)

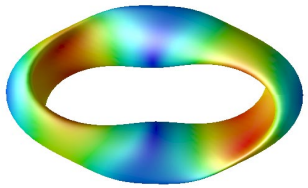

Bootstrap current

– Weak shear with iota mainly from coils

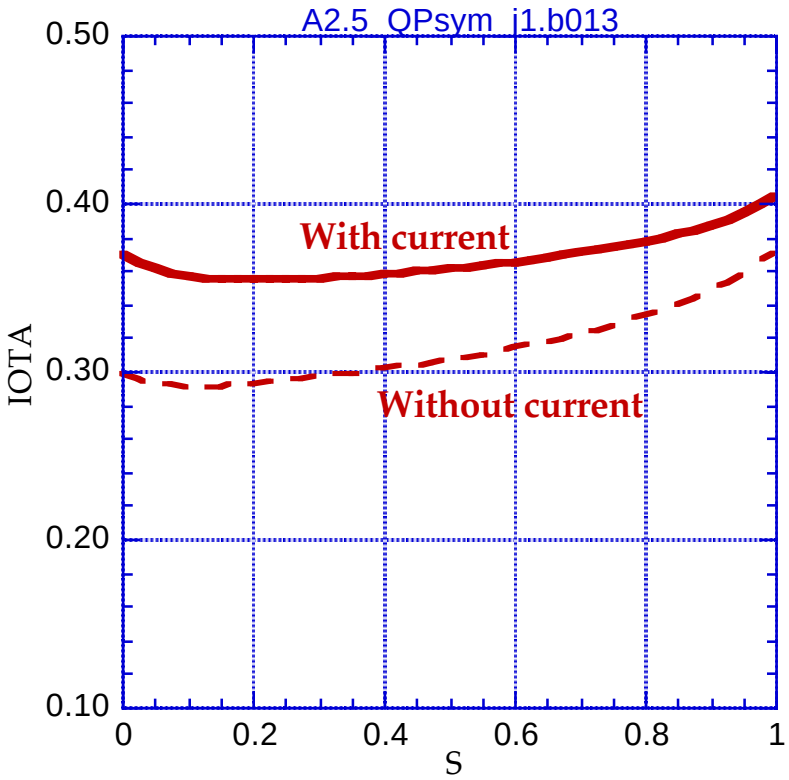

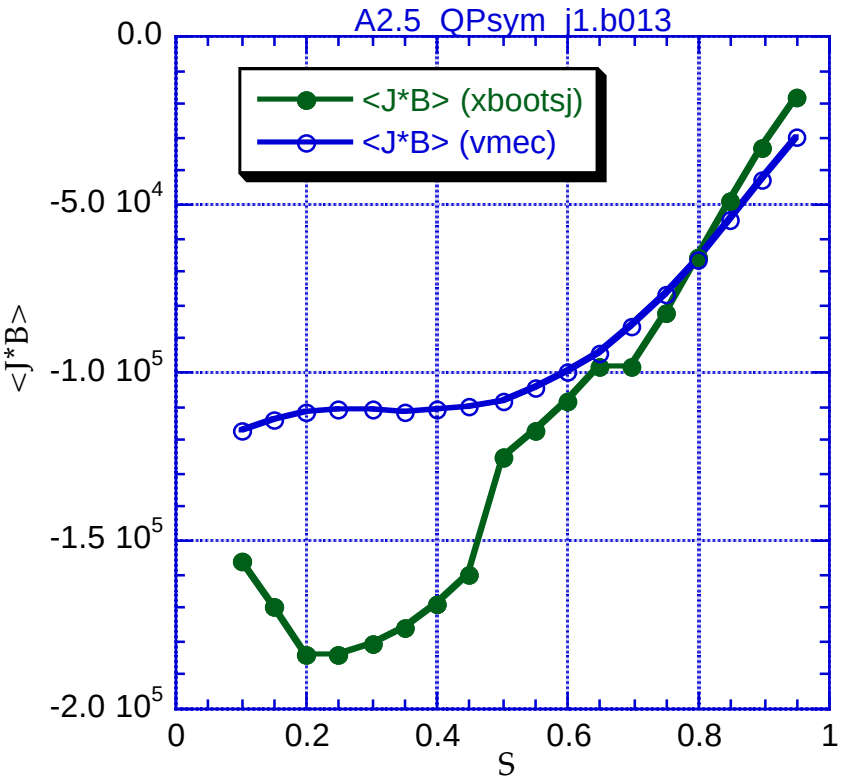

– Bootstrap consistency is fair

QP Symmetry Cases (cont.)

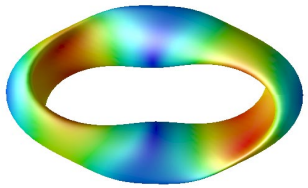

Stability

– Pressure profile for this case is ballooning unstable

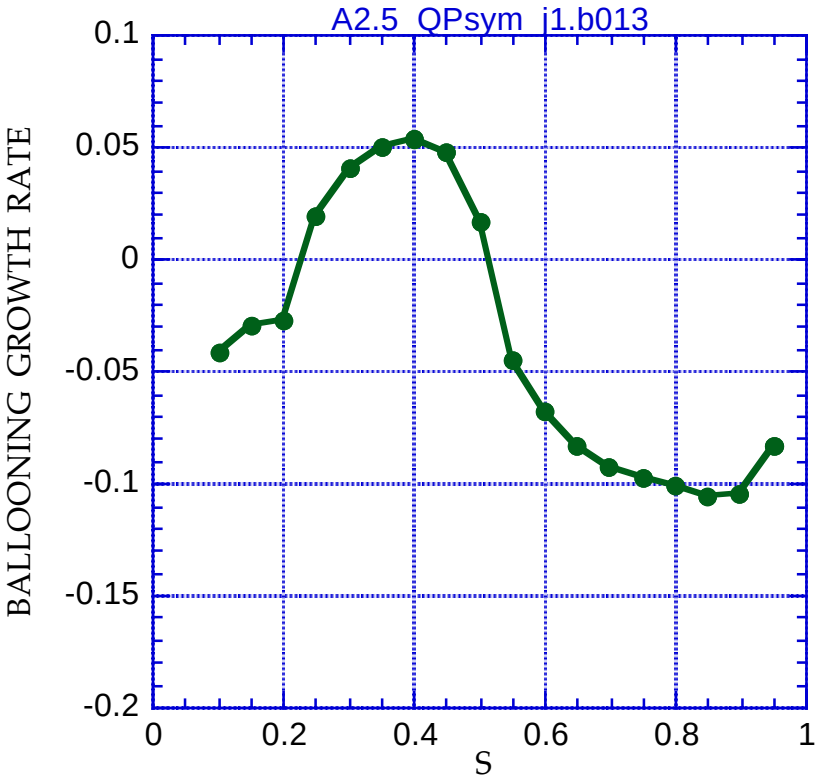

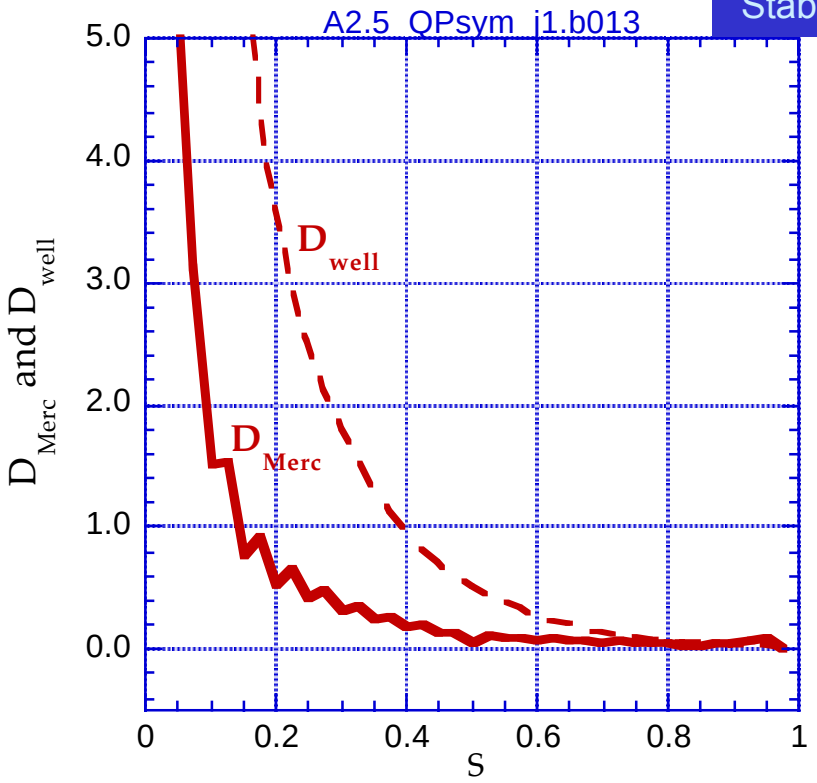

– Mercier stable due to the well at the center

QP Symmmetry Cases (cont.)

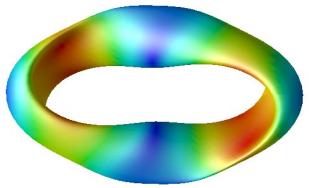

– Modifying the pressure profile however....

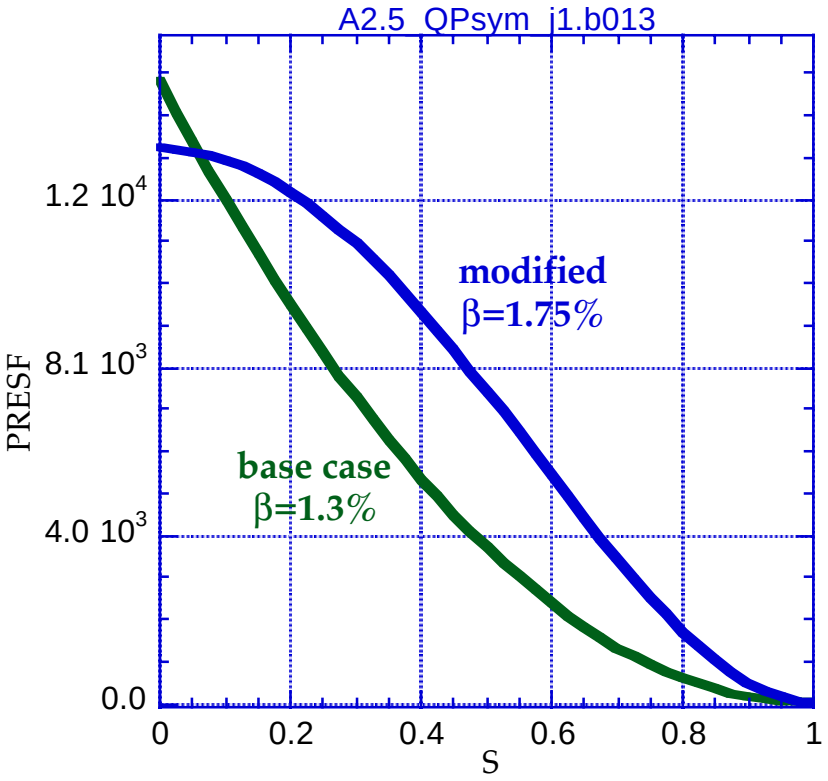

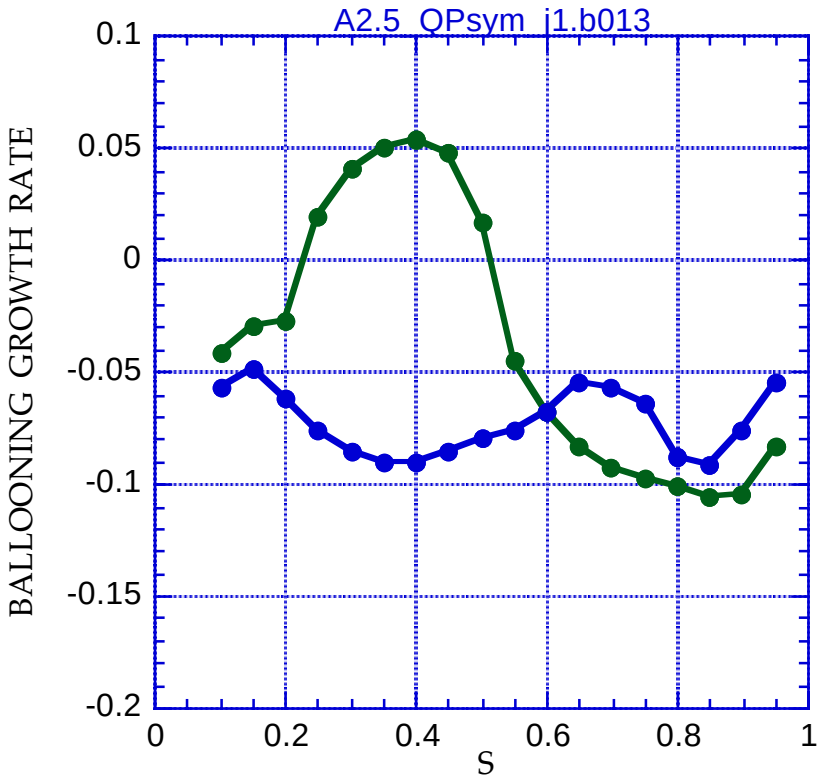

– ... leads to ballooning stability at higher β

PIES Flux Surfaces at β = 1.6%

Flux surface fragility

Fixed Boundary

Free Boundary

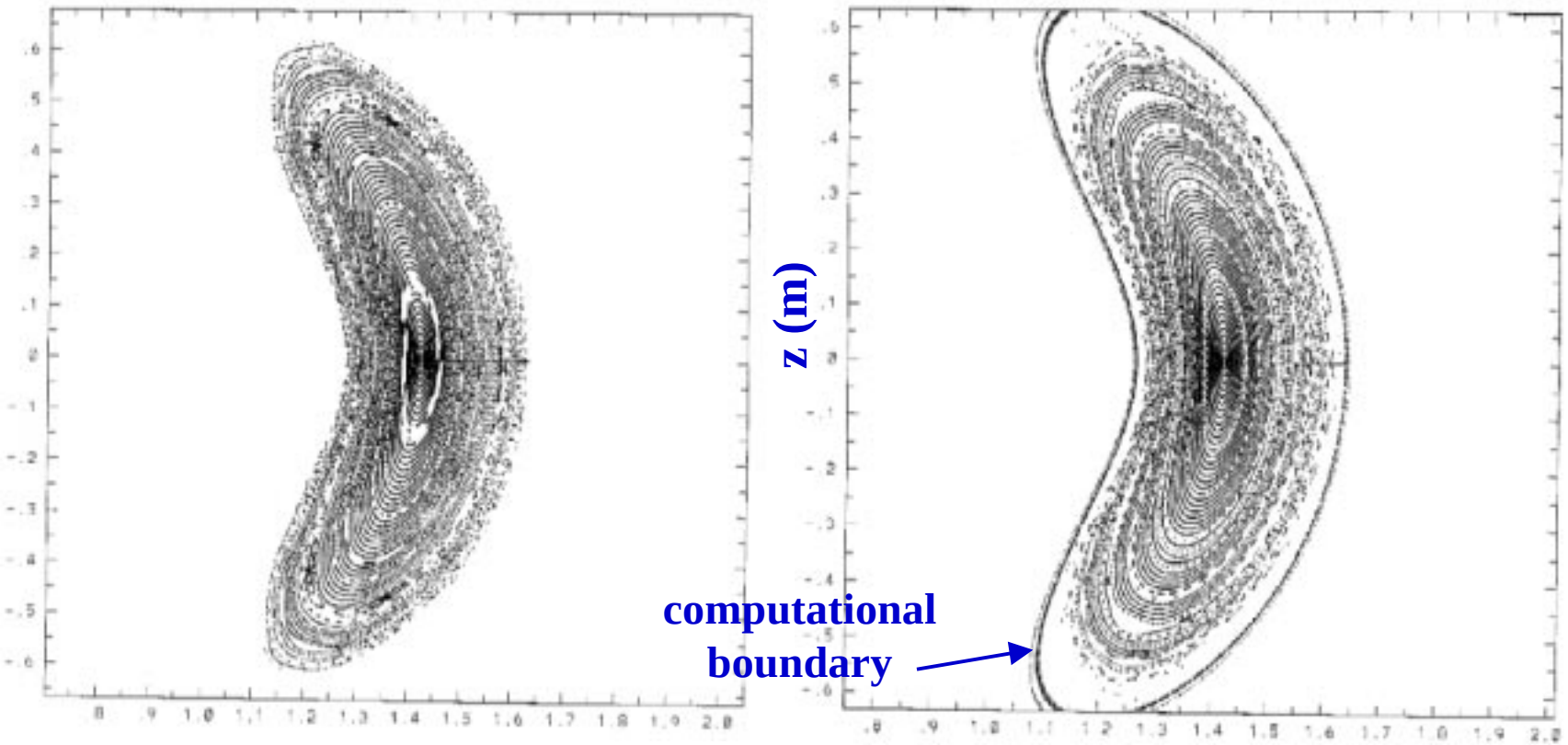

D. Monticello

High β Configurations

Equilibrium

- A class of configurations with high β MHD stability limits
  - Rotational transform primarily from plasma current
  - Better alignment with self-consistent bootstrap current than advanced tokamaks
  - Stable at higher β than comparable tokamak due to lower current

High β Configurations (cont)

- Have obtained 3 field period configurations with ballooning stability up to β=23%, Vertical/Kink stability up to β =15% (G. Fu),
  aspect ratios A~3.5 - 4.5
- For lower aspect ratio (A~2.7) 2 field period devices, testing effect of lowering elongation and boosting external rotational transform on vertical stability

High β Case: 3 Field Periods

Equilibrium

– Outer flux surface/cross sections: 3 FP, A=3.7, β=15%

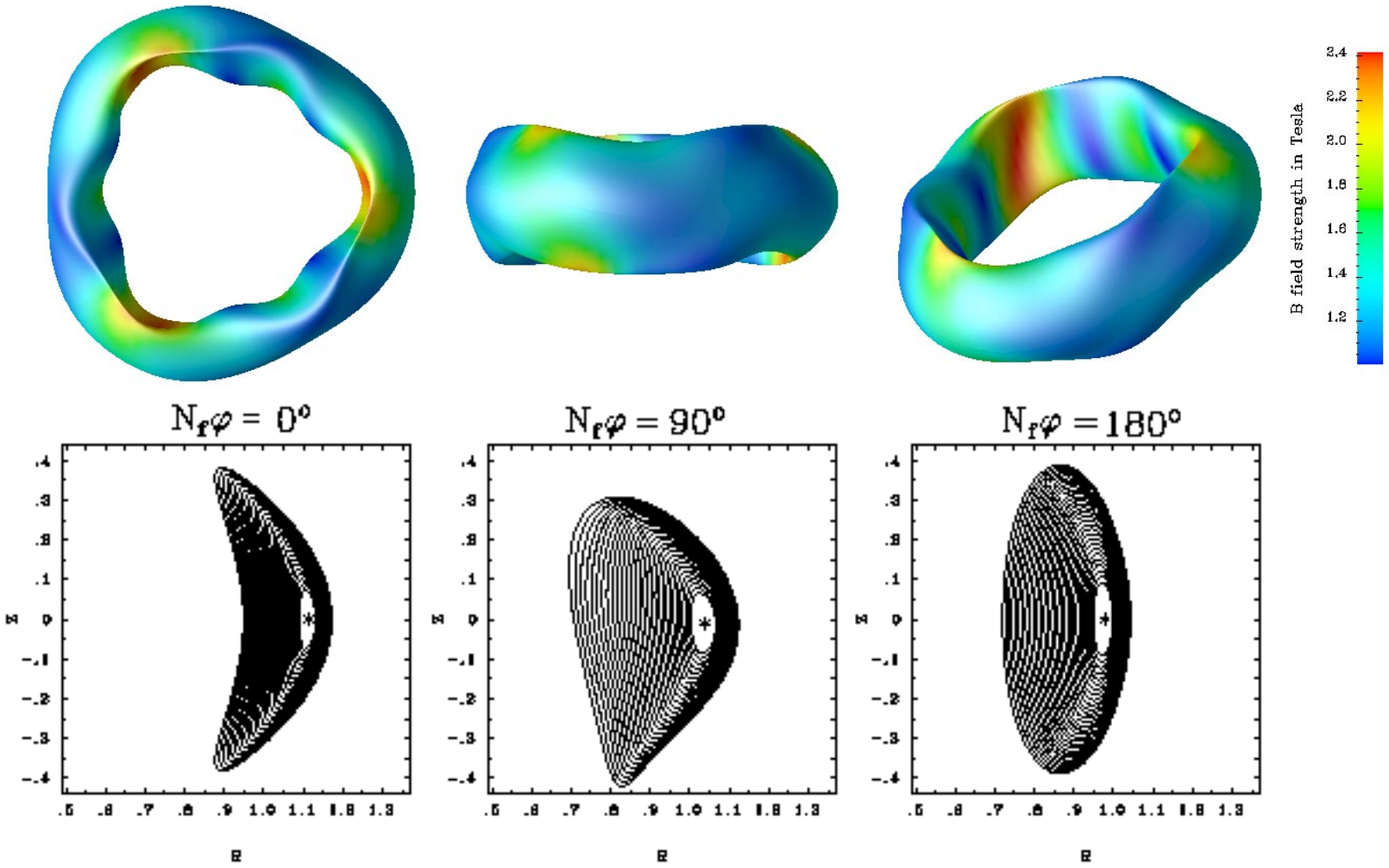

High β Case: 3 Field Periods

Bootstrap current

– 3 FP, A=3.6, β=15%, <|B|>=1 T, Max.Tor.Cur.= 155 kA

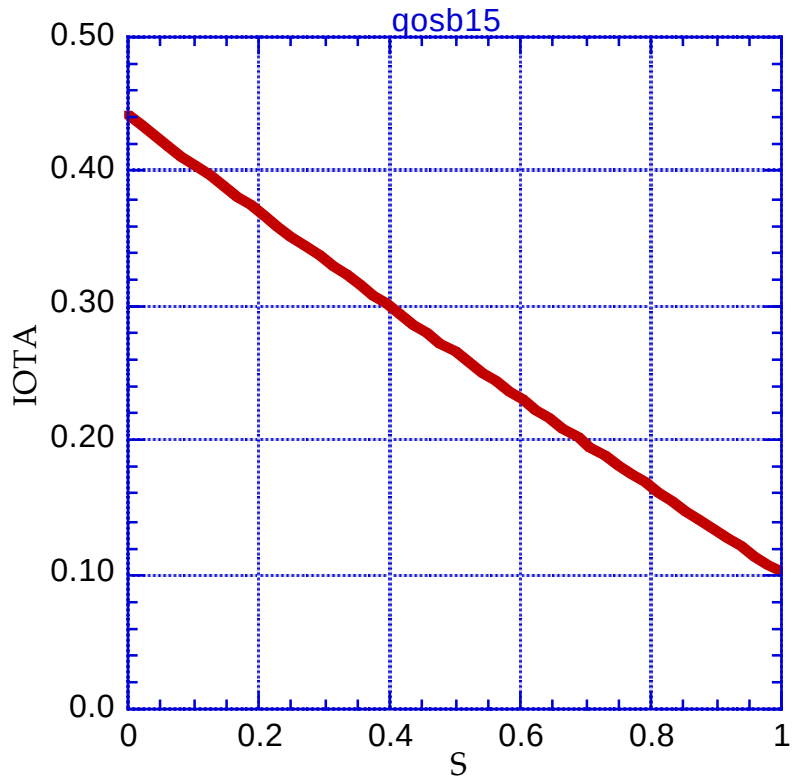

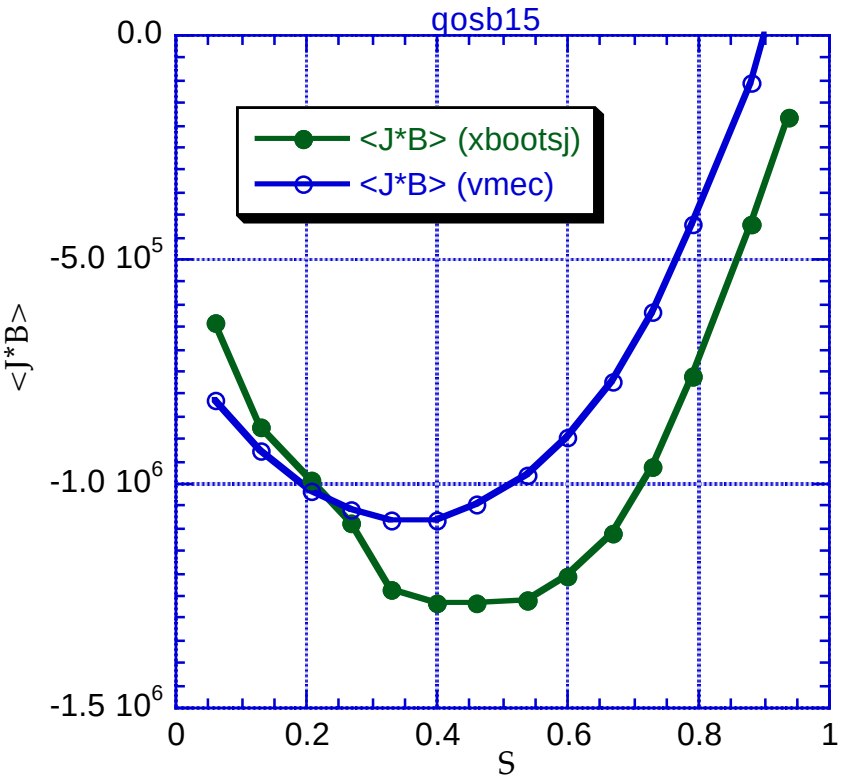

Variation of B_{mn} Spectra for type II Configurations with <β>

Equilibrium

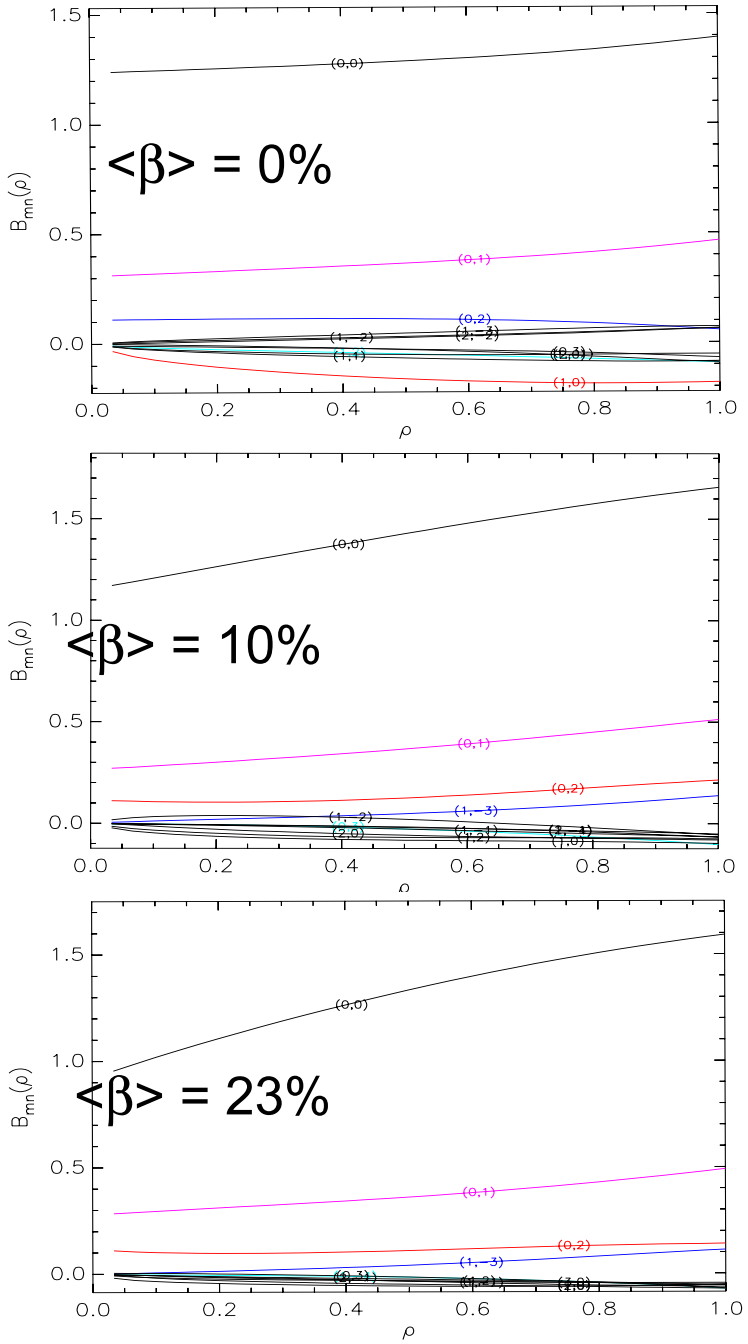

High β Case: |B|/Flux Surface Alignment

- |B| surfaces align with flux surfaces at higher b:

β=0%:

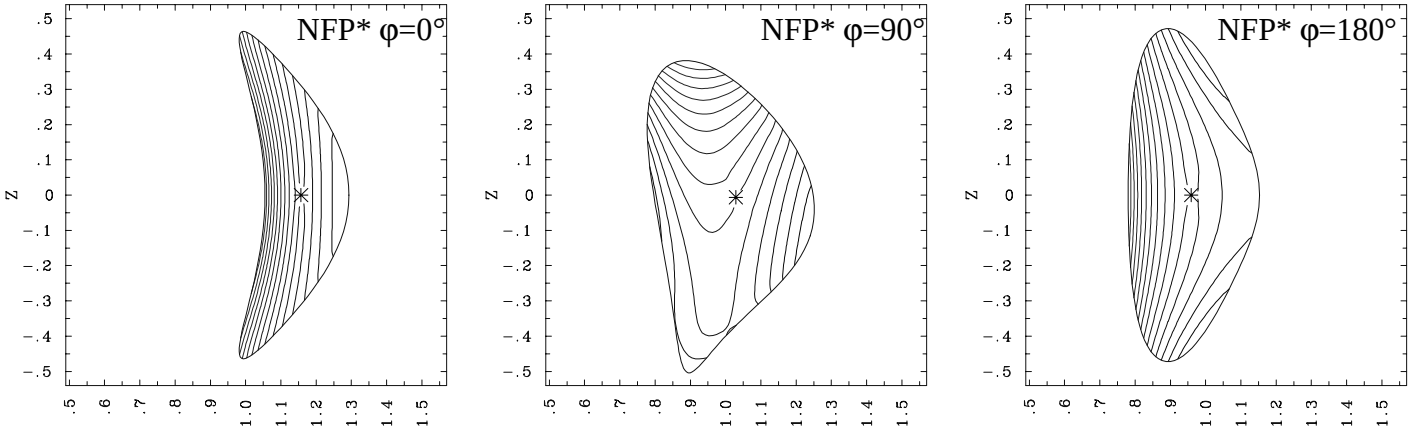

β=23%:

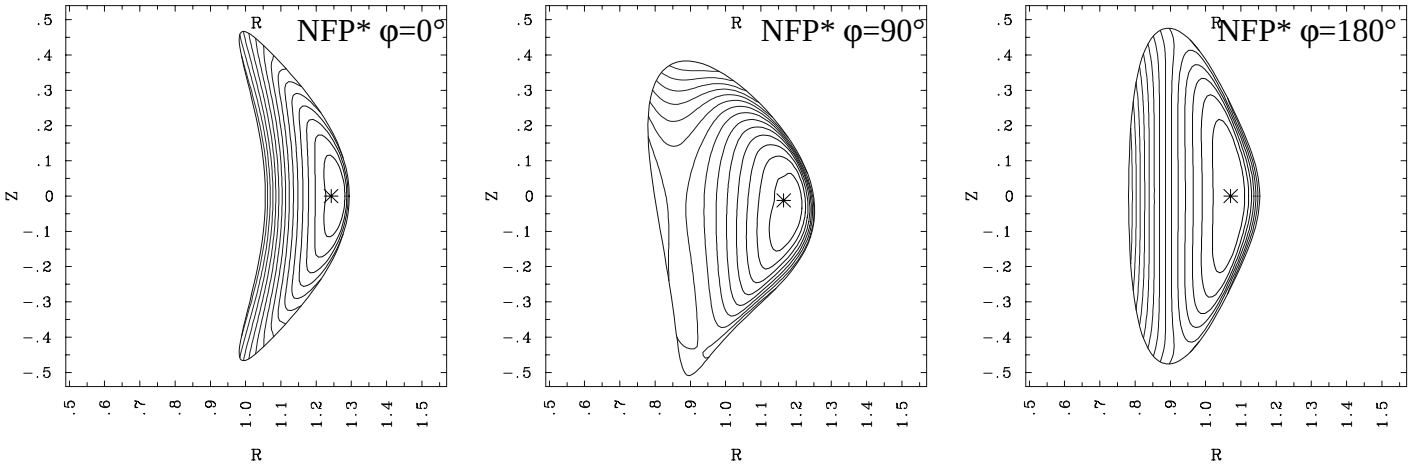

|B| contours for type II configurations show a significant improvement in poloidal symmetry with increasing <β>

Equilibrium

<β> = 0%

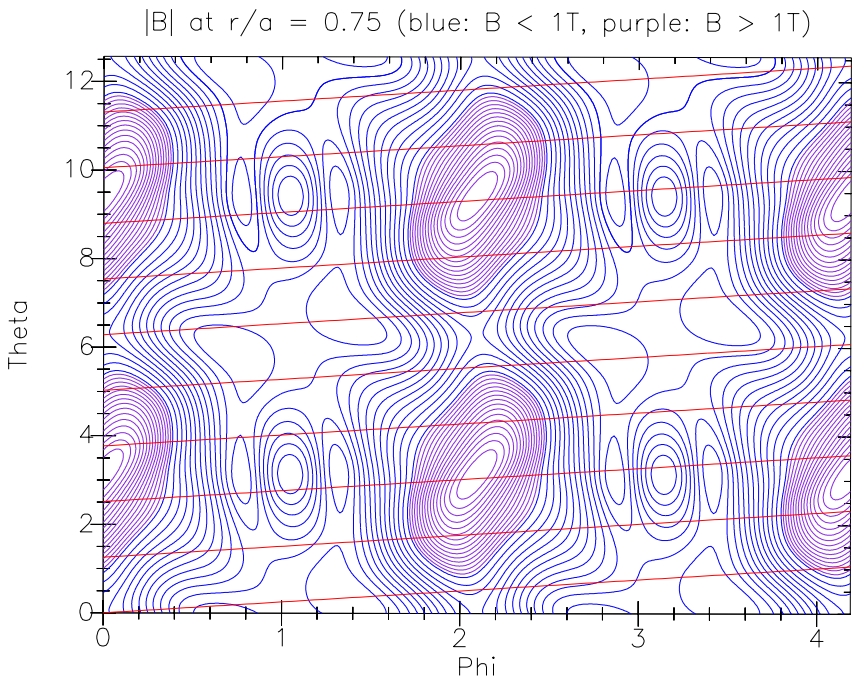

<β> = 23%

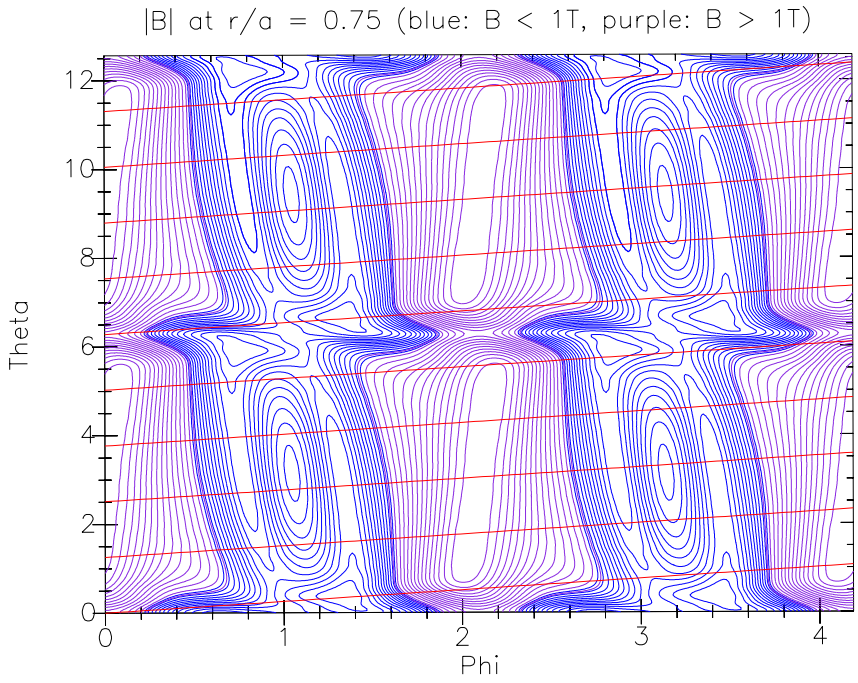

Through its modification of |B|, high β changes both the thermal neoclassical transport and bootstrap coefficient

Monte Carlo calculation of energy lifetimes

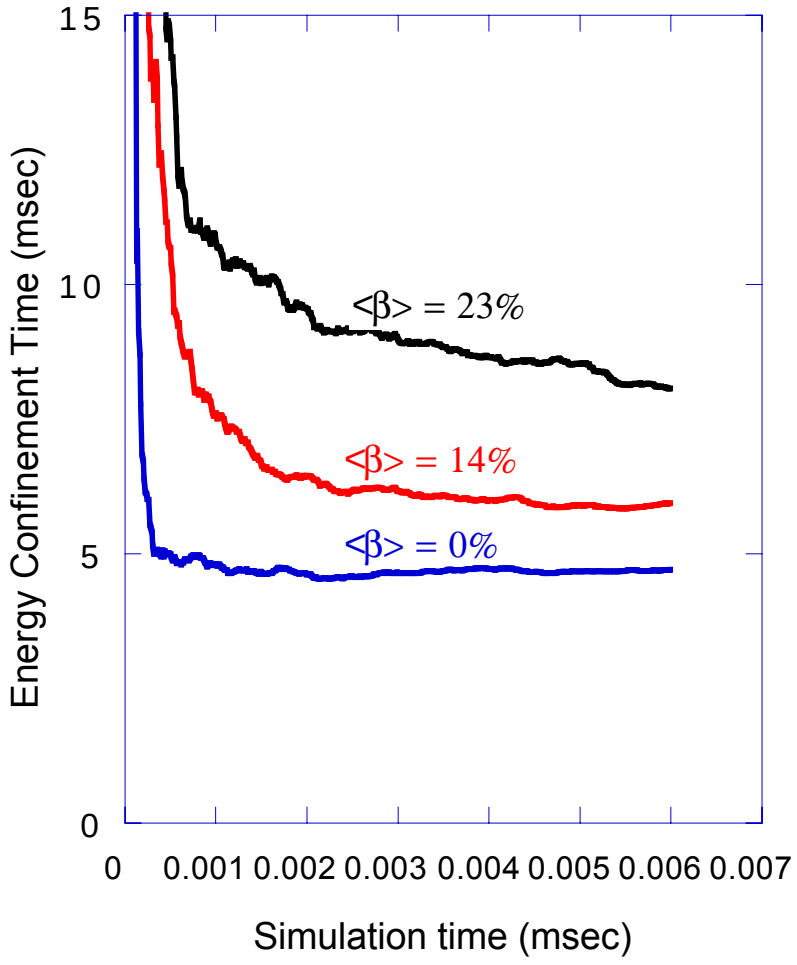

DKES calculation of L_{31} bootstrap coefficient

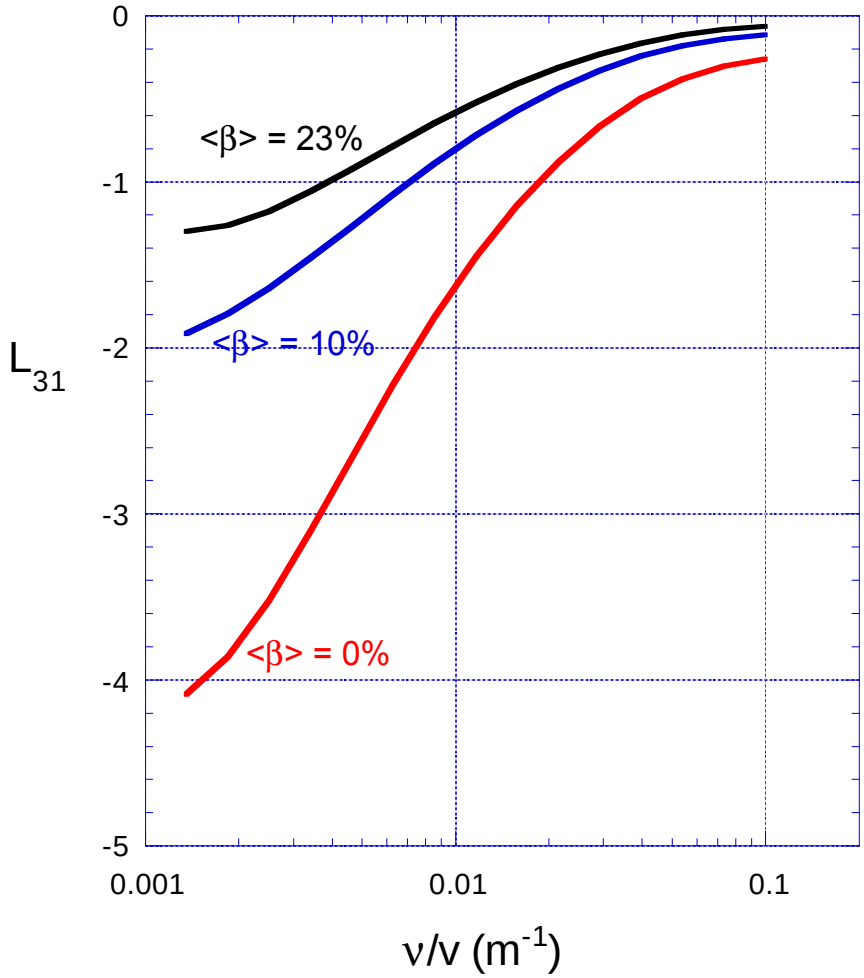

Increasing β leads to improved neoclassical transport and to a decreased bootstrap current coefficient.

(results shown are for 3 field period, A = 3.4 device)

Transport analysis

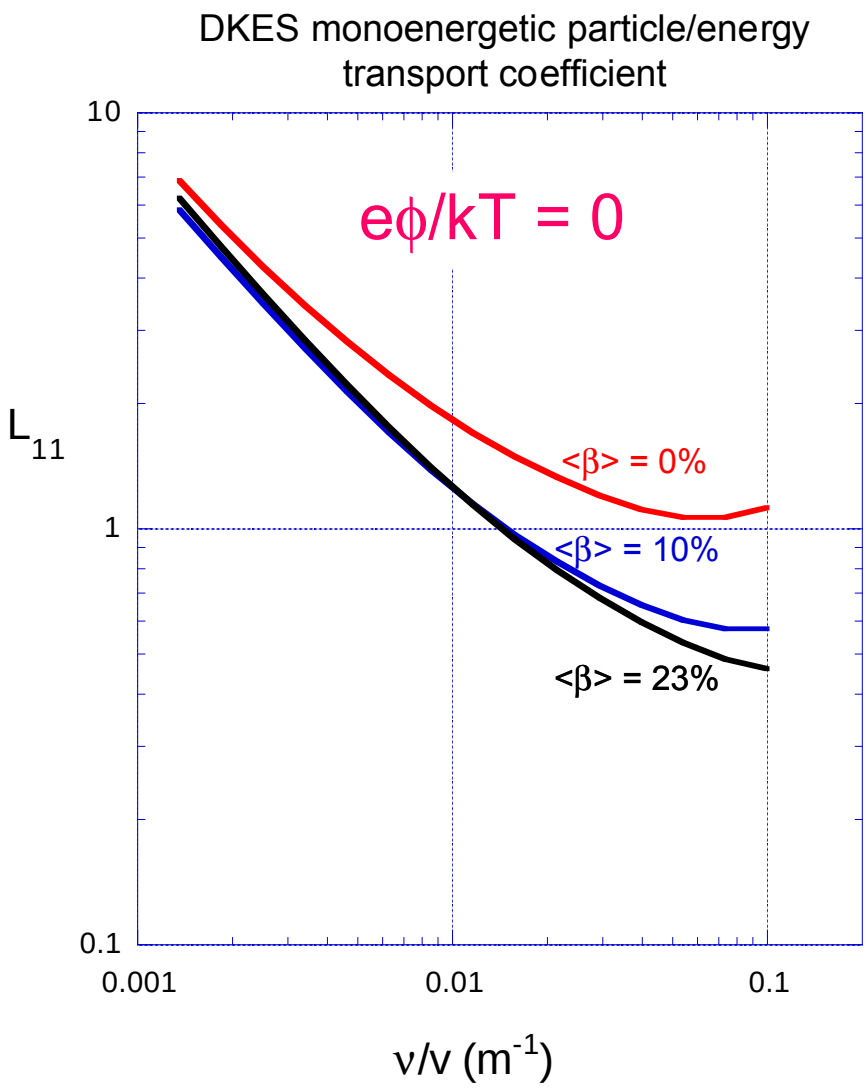

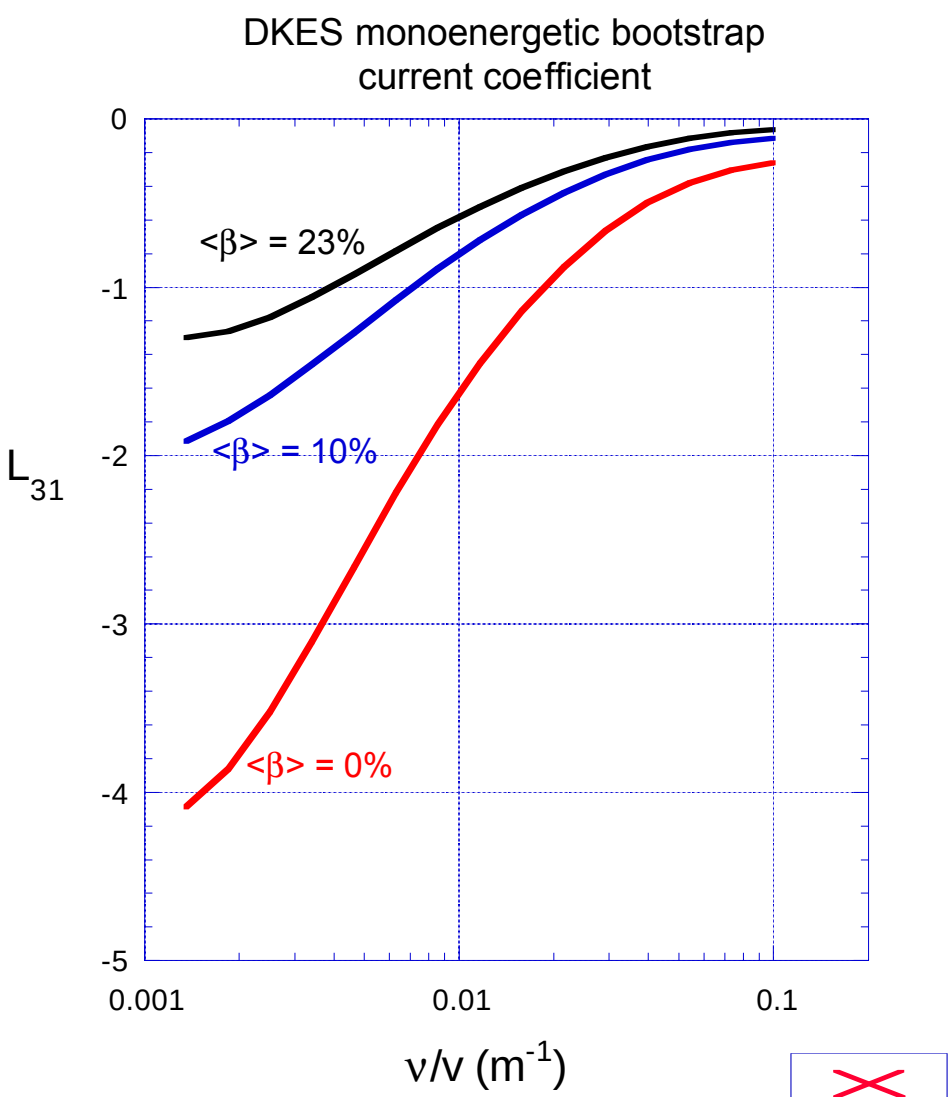

α-particle slowing-down simulations show these devices indicate very good confinement with increasing β.

Transport analysis

The configuration was scaled to <B> = 5T and R_0 = 10m for alpha confinement studies

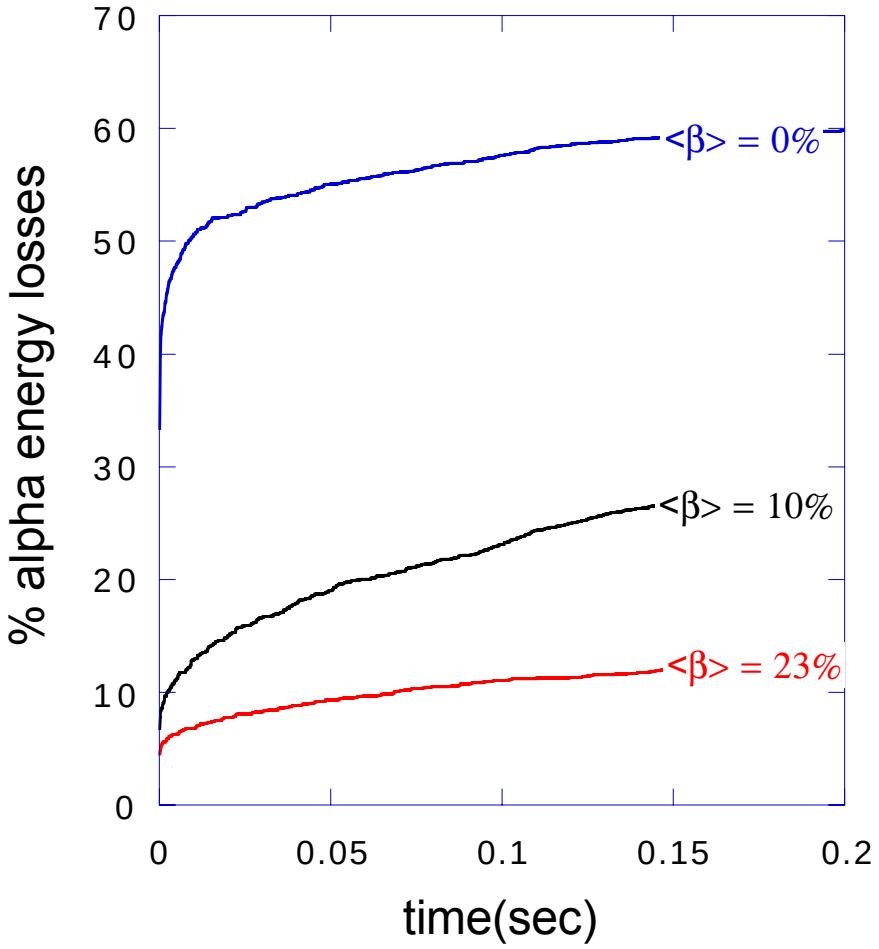

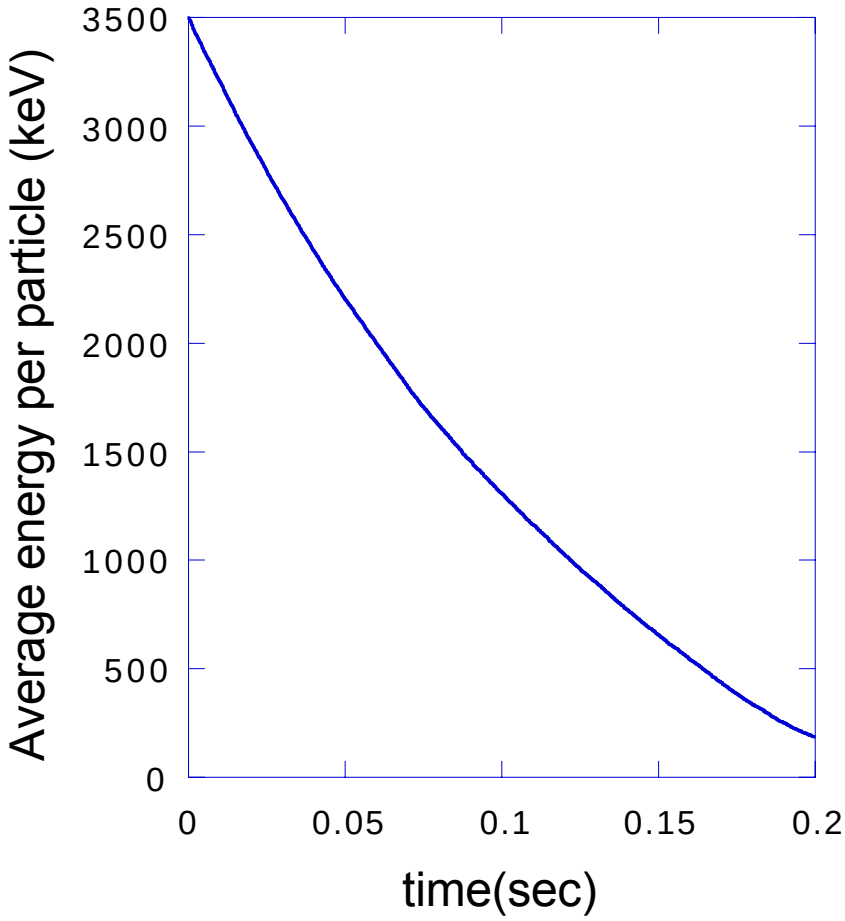

High β Case: Ballooning Stability

- For the 3 FP, β=15%, A=3.7 case: (R. Sanchez)
- Edge becomes ballooning unstable for <β> >0.25%, Second regime stabilization begins at edge above <β > = 0.6%, and stabilizes it beyond 1%.
- The region of the plasma in second regime moves inwards from the edge for increasing < β >.
- Plasma becomes totally stable above < β > = 7%
- Innermost part of the plasma always in first stability regime.

High β Case: 2 Field Periods

Equilibrium

– Outer flux surface/cross sections: 2 FP, A=2.7, β=5%

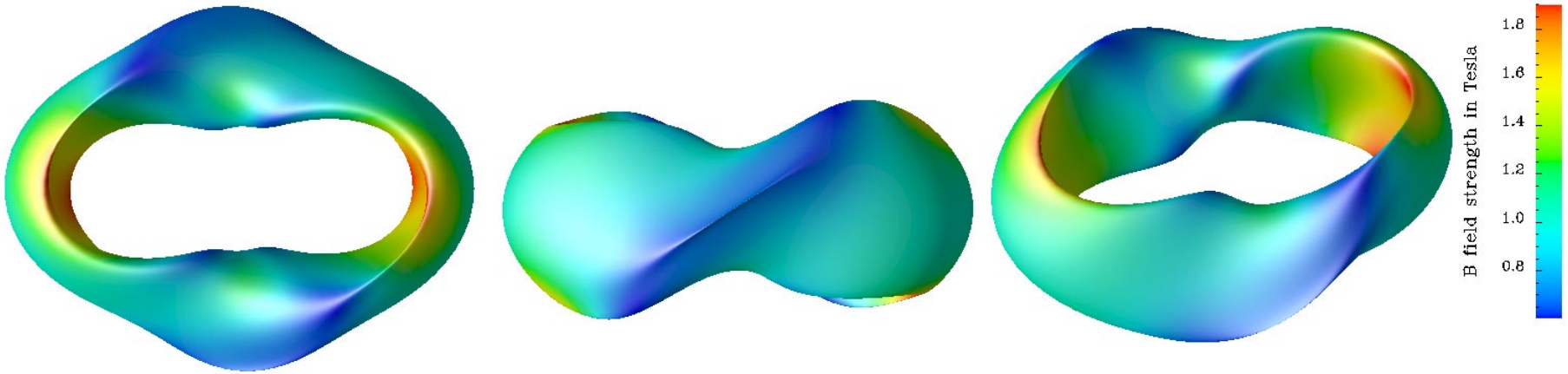

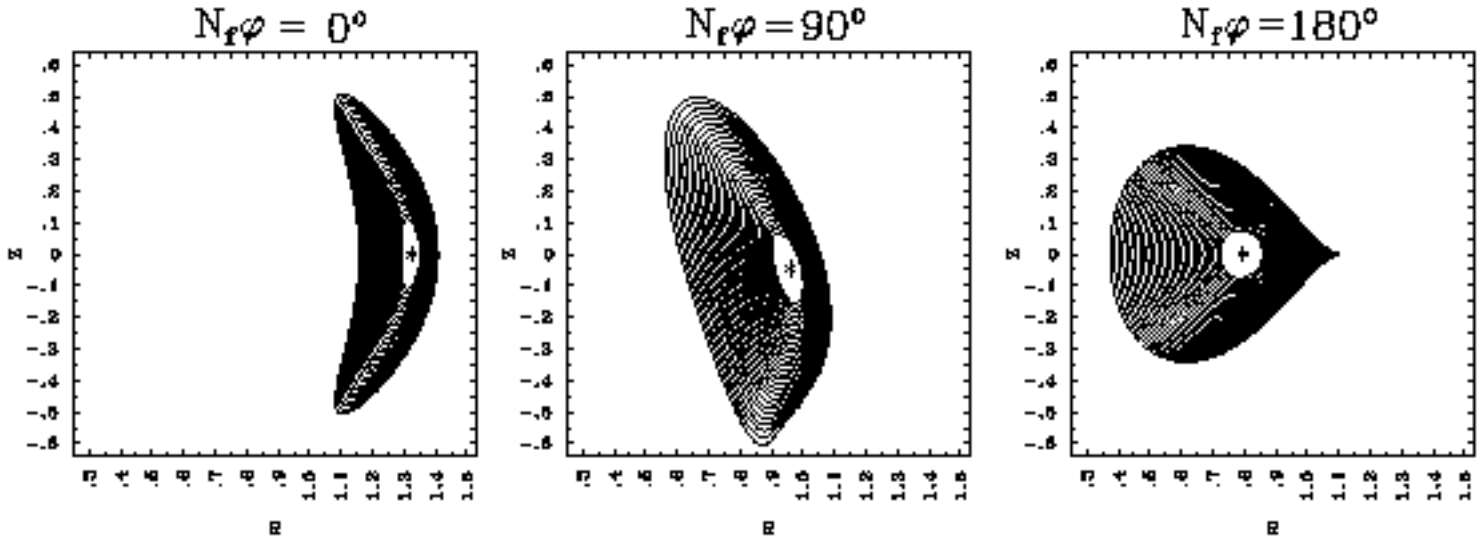

High β Case: MHD Stability

Bootstrap current

– Have been able to affect the stability by increasing the amount of external transform (Fu)

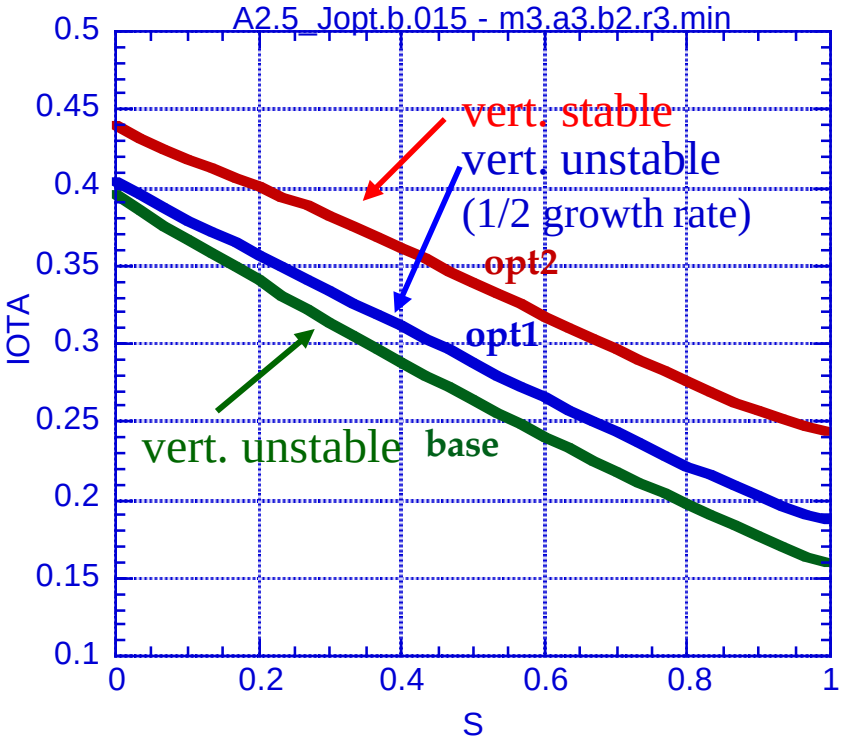

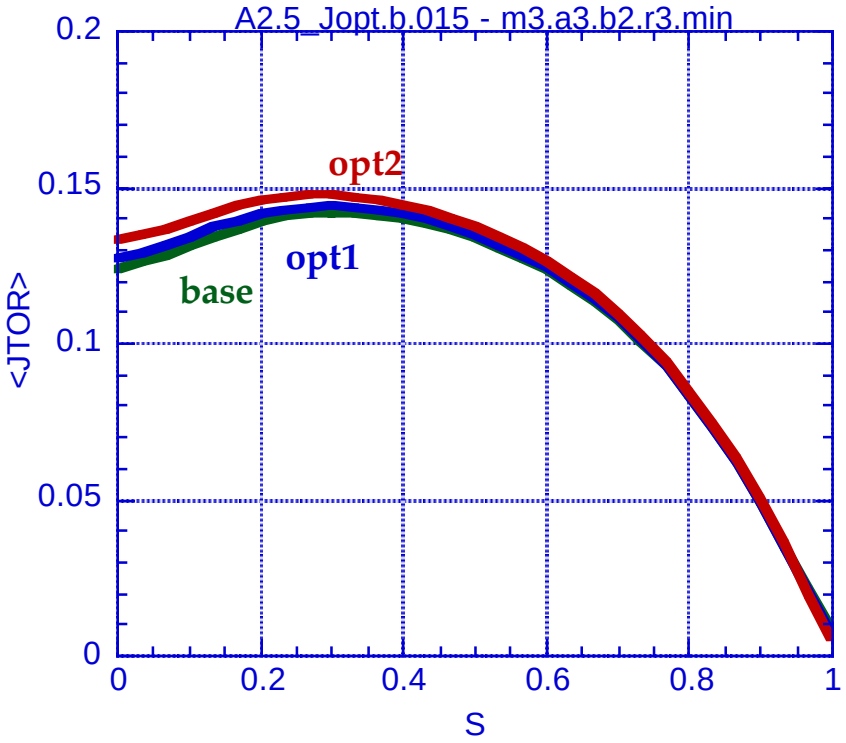

STABILITY REGIMES

- Edge becomes ballooning unstable above $<\beta> = 0.25\%$.
- Second regime stabilization begins to be effective at edge above $<\beta> = 0.6\%$, and stabilizes it beyond 1%.
- The region of the plasma in second regime moves inwards from the edge for increasing $<\beta>$.
- Plasma becomes totally stable above $<\beta> = 7\%$
- Most inner part of the plasma stays always in first stability regime.

BALLOONING SPECTRUM (LOW-β)

Stability

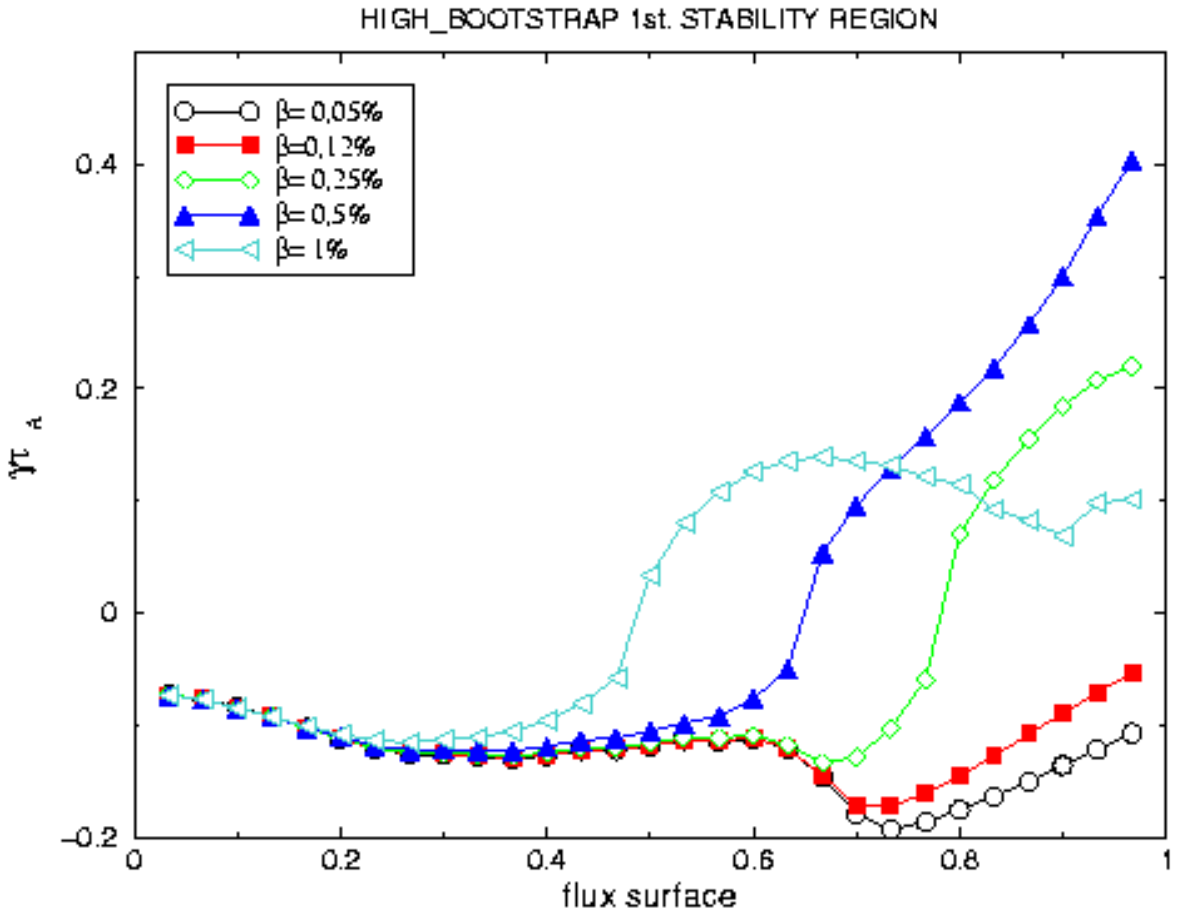

BALLOONING SPECTRUM (HIGH – β)

Stability

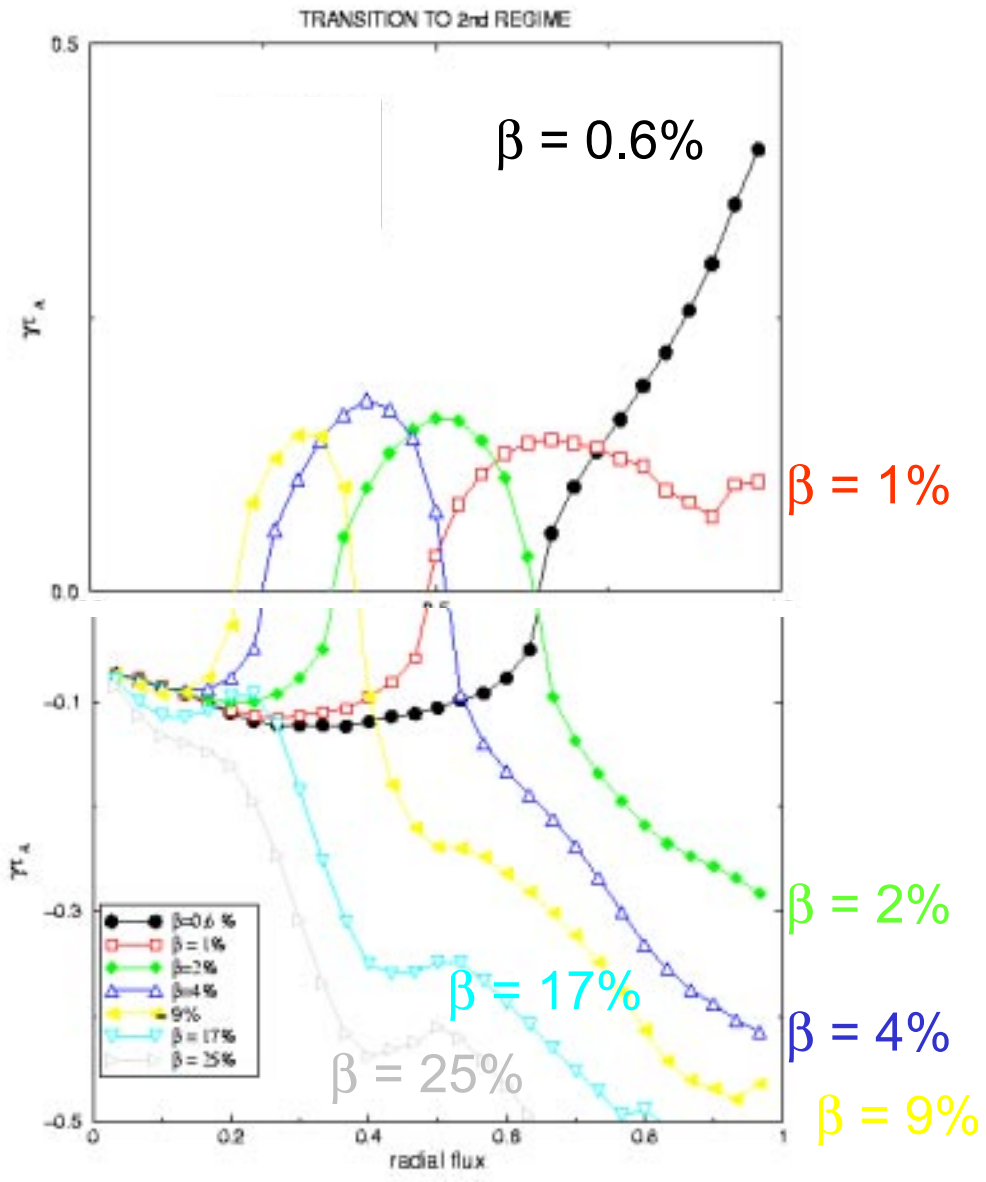

MERCIER STABILITY

- Plasma remains Mercier stable except for a range of $<\beta>$ between 3-6%.
- Mercier modes are stabilized due to the existence of a large magnetic well that increases with $<\beta>$.
- The radial region of instability is identical to the region of ballooning instability for the same values of $<\beta>$
- This might help to optimize both type of unstable modes in the same way.

MERCIER STABILITY

Stability

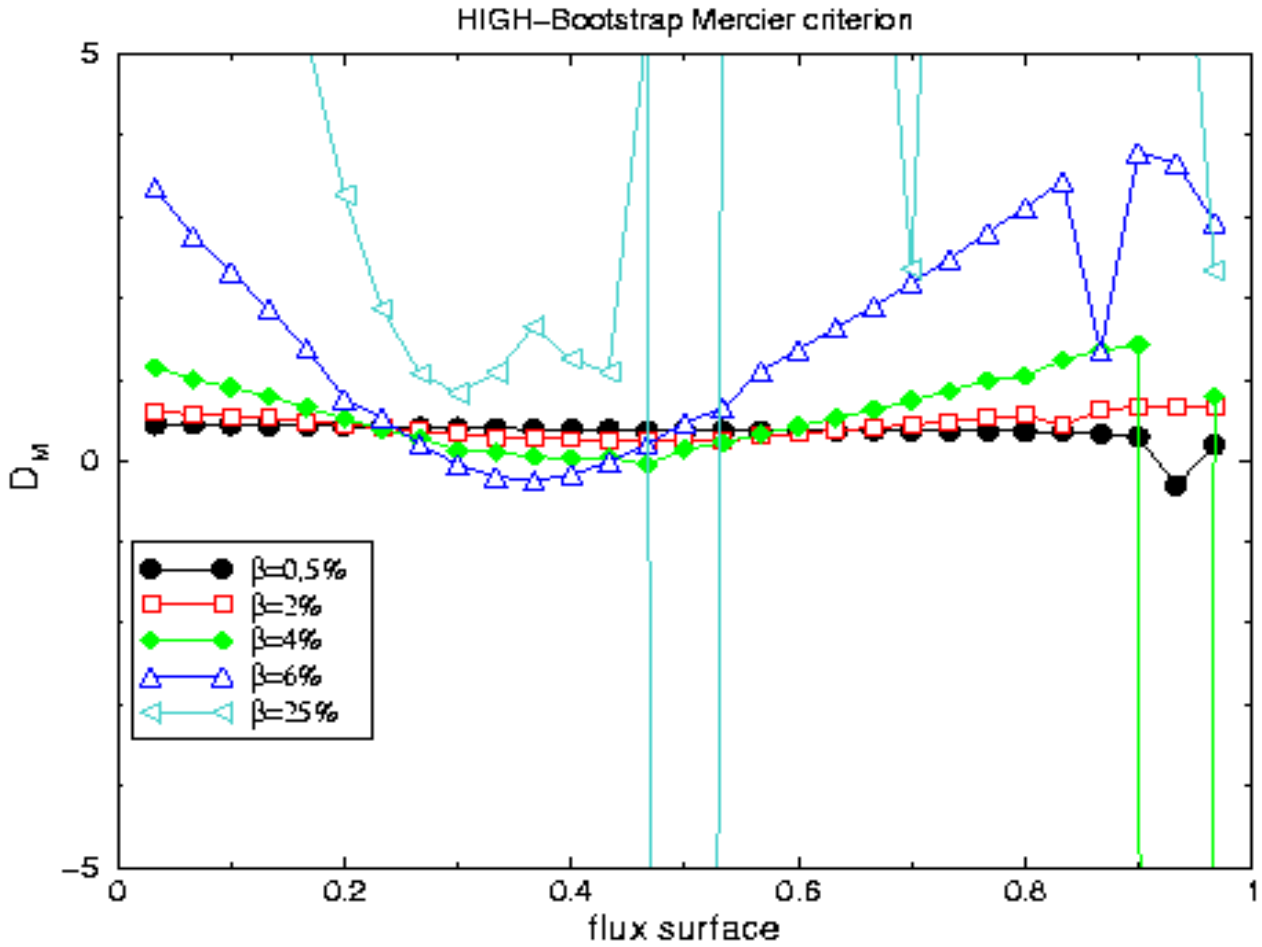

Summary

- Attractive 2 and 3 field period devices have been found for A = 2.5 - 3.5
  - Attain good confinement by being near quasi-poloidal symmetry
  - Modular coils: good flux surface reconstruction, preserves physics
- Different heating options and magnetic field variation (0.5 – 1T) allow exploration of different confinement regimes
  - ECH: τ_{neo}/τ_{ISS95} from 1.4 to 2
  - ICH: τ_{neo}/τ_{ISS95} from 3 to 3.6
- Quasi-poloidal symmetry minimizes viscous damping in the direction of the E_r x B drifts
  - lower parallel flows
  - influences accessiblity of enhanced confinement regimes which rely on E_r x B shear

Summary (contd.)

- High β configurations offer improved confinement with increasing β
  - Large fraction of the transform from plasma current
  - Similar to advance tokamak, but bootstrap current is well aligned and not too large (as it is in an axisymmetric device)
  - Stability limits (ballooning, kink, vertical) allow operation at $\langle\beta\rangle \sim 15\%$ (second regime stability)
  - Have achieved lowest alpha losses (~12%) of any of our configurations